Solvent-Controlled Switch of Selectivity between sp^2 and sp^3 C–H Bond Activation by Platinum (II)

By

Alexander William Garner

November, 2010

Chair: Dr. Rickey Hicks

Major Department: Chemistry

Cyclometalation reactions have been studied intensely for the past few decades, especially those containing palladium. The factors that control the process of the C-H bond activation, however, are not yet completely understood. C-H bonds are ever-present in organic molecules, but the vast majority of them cannot be exploited for chemical reactions due to their inert and stable nature. Early attempts to activate these bonds led to very complicated mixtures of products, and therefore not an acceptable means of C-H activation due to poor selectivity. Controlling the selectivity of a reaction is one of the most important issues surrounding synthetic chemistry. It is generally recognized that aromatic C-H bonds are more likely to undergo activation by platinum complexes. However, recently it has been illustrated that there is a delicate balance between sp^2 and sp^3 C-H bond activation in a platinum (II) complex system.

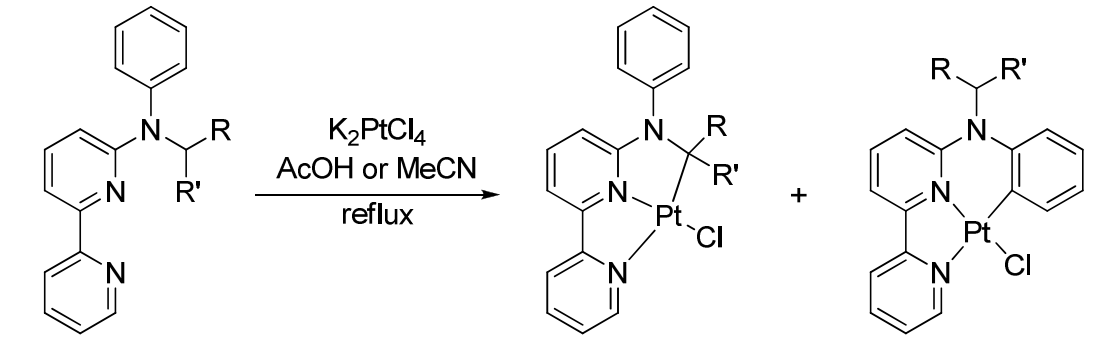

R = R' = H (**L1**)
R = CH_3, R' = H (**L2**)
R = R' = CH_3 (**L3**)

R = R' = H (**1A**)
R = CH_3, R' = H (**2A**)
R = R' = CH_3 (**3A**)

R = R' = H (**1B**)
R = CH_3, R' = H (**2B**)
R = R' = CH_3 (**3B**)

In this study, the solvent-controlled switch of selectivity between sp^2 and sp^3 C-H bond activation in platinum (II) complex systems will be discussed. Ligands **L1** through **L3** were designed and synthesized to test the selectivity of cycloplatination of a reaction with potassium tetrachloroplatinate (II) in two different solvents, acetonitrile and glacial acetic acid. It was found that in each of the solvents used, a different isomer was produced from the complexation reaction. Reactions of **L1** through **L3** with potassium tetrachloroplatinate (II) in acetonitrile produced the sp^2 substituted isomer (**1B**-**3B**), while the same reaction performed in glacial acetic acid formed the sp^3 substituted isomer (**1A**-**3A**). It was determined through mechanistic studies that the sp^2 substituted isomer is a kinetically controlled product, while the sp^3 substituted isomer is a thermodynamically controlled product. Also, it was found that the ratio of products depends on time, where as more time goes by the thermodynamically stable product begins to predominate.

Other issues examined in this study were the side reactions that occurred during the complexation of ligands **L2** and **L3**. These side products were due to C-C bond cleavage in **L2** and C-N bond cleavage in **L3**. These side products were characterized and studied in their own right.

Solvent-Controlled Switch of Selectivity between sp^2 and sp^3 C-H Bond Activation by Platinum (II)

A Thesis

Presented to

The faculty of the Department of Chemistry

East Carolina University

In Partial Fulfillment

Of the Requirements for the Degree

Masters of Science in Chemistry

by

Alexander William Garner

November, 2010

Solvent-Controlled Switch of Selectivity between sp^2 and sp^3 C-H Bond Activation by Platinum (II)

by

Alexander William Garner

APPROVED BY:

DIRECTOR OF THESIS:_____

Dr. Shouquan Huo

COMMITTEE MEMBER: _____

Dr. Brian Love

COMMITTEE MEMBER: _____

Dr. Yu Yang

COMMITTEE MEMBER:_____

Dr. Libero Bartolotti

COMMITTEE MEMBER: _____

Dr. Yong-Qing Li

CHAIR OF THE DEPARTMENT OF CHEMISTRY: _____

Dr. Rickey Hicks

DEAN OF GRADUATE SCHOOL: _____

Dr. Paul Gemperline

TABLE OF CONTENTS

LIST OF FIGURES

LIST OF SCHEMES

LIST OF TABLES

LIST OF ABBREVIATIONS

π	Bonding orbital
π^*	Anti-bondong orbital
^0C	Centigrade
Å	Angostroms
AcOH	acetic acid
DFT	Density Functional Theory
DPPF	Diphenylphosphino Ferrocene
HOMO	Highly Occupied Molecular Orbital
h	Hours
IL	Intra ligand
LUMO	Least Unoccupied Molecular Orbital
MLCT	Metal to Ligand Charge Transfer
MC	Metal Centered
mmol	milli moles
NMR	Nuclear Magnetic resonance
$Pd(dba)_2$	Paladiumdibenzyledene acetone
TLC	thin layer chromatography
dmso	Dimethyl sulfoxide
HMPA	Hexamethylphosphoramide
GC-MS	Gas chromatography-mass spectrometry
Q-TOF	Quadrupole-time of flight mass spectrometer
MHz	Megahertz

NaO^tBu	Sodium tert-butoxide
Ppm	Parts per million
CuI	Copper Iodide
CH_2Cl_2	Dichloromethane
rt	Room temperatrue
CH_3CN	Acetonitrile

CHAPTER 1: BACKGROUND

The design and synthesis of phosphorescent transition metal complexes have gained much attention in recent years. The interest in these particular types of complexes started from the $[Pt(tpy)Cl]^+$ (**I**) complex, which was first synthesized in 1934.[1]

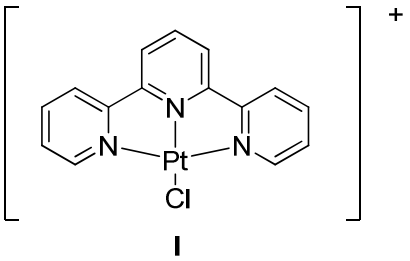

I

Figure 1: The first platinum complex (**I**)

In the 1970's, there was a renewed interest shown in platinum complexes as DNA intercalators.[2] However, the early 1990's was the first time that the excited state and luminescence properties of Pt(II) complexes were investigated in detail, yielding a wealth of interesting systems with a rich variety of emissive excited states, which were tuned by adjusting the structures of the ligands.[3] The drawback of complexes using this terpyridine is that the angle of the N-Pt bond is not ideal for second and third row transition metal ions. The two lateral Pt-N bond lengths are usually lengthened beyond their ideal values due to the constraints imposed by the rigidity of the ligand. Due to this bond lengthening, the ligand field is reduced, and the d-d excited states that promote thermally activated nonradiative decay are lowered in energy.[4]

Complex I, however, is neither an organometallic compound nor a cyclometalated complex due to a lack of Pt-C bonds. Cyclometalation is an important process used in organometallic chemistry, which refers to the activation of the C-H bond by transition metal

catalysts, a chelation-assistance strategy.[5] Many of the cyclometalated complexes are highly stable, and can be isolated and characterized. These qualities make them extremely important for studies relating to the fundamental issues regarding the C-H activation.[6]

There are typically three classes of cyclometalated platinum complexes: bidentate, tridentate, and tetradentate complexes.

Bidentate Complexes

Bidentate complexes can be further categorized into two types, homoleptic and heteroleptic complexes. These complexes are illustrated in **Figure 2** below.

Homoleptic Complexes

Homoleptic complexes are composed of two identical ligands like the bis-cyclometalated complex *cis*-$Pt(ppy)_2$ (ppy = mono anionic 2-phenylpyridine ligand).[7] However, these bidentate complexes are nearly non-emissive at room temperature.[8] Another homoleptic bidentate platinum complex, $Pt(thpy)_2$ (thpy = mono anionic 2-(2-thienyl)pyridine ligand), was studied and found to be emissive at room temperature[8] but unstable toward sublimation, making it unsuitable for the vapor deposition process required for producing highly efficient small molecule organic light emitting diode (OLED) devices.[9]

Heteroleptic Complexes

Heteroleptic complexes contain two different coordinating ligands. These mono-cyclometalated complexes have the generic formula (ppy)PtL[10] where L is an ancillary ligand such as acetylacetonate or picolinate. One example of this type of complex is Pt(ppy)(acac), as illustrated below in **Figure 2**. Other examples of heteroleptic complexes are: $[Pt(N\hat{}C)(N\hat{}N)]^+$,

$[Pt(N^C)Cl_2]^-$,[11] and $[Pt(N^C)(CO)SR]^-$.[12] These heteroleptic complexes are emissive at 77K and at room temperature.

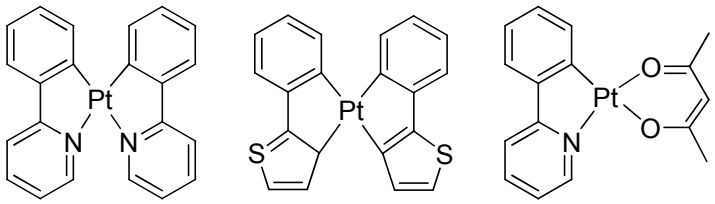

cis-$Pt(ppy)_2$ $Pt(thpy)_2$ Pt(ppy)(acac)

Figure 2: Prototypes of bidentate platinum complexes

Tridentate Complexes

The rigidity of cyclometalated complexes tends to favor phosphorescence over the non-radiative paths of decay. Bidentate complexes tend to undergo plane distortion which affects their emissive properties at room temperature. For this reason, tridentate complexes were developed to enhance the rigidity of the ligands, which do not distort as much as bidentate complexes. Much interest has been paid to the tridentate cyclometalated complexes such as those derived from tridentate C^N^N (6-phenyl-2,2'-bipyridine),[13] C^N^C (2,6-diphenylpyridine),[14] and N^C^N (1,3-dipyridylbenzene)[15] ligands.

Pt(C^N^N) Complex

Much of the published work regarding these complexes has been pioneered by Che and Lai.[16] The complex with this coordination can be prepared by complexing the ligand, 6-Phenyl-2-2'-bipyridine (phbpyH) with K_2PtCl_4. This complex is illustrated in **Figure 3**. This ligand

contains a phenyl group on one side of the ligand. This complex is emissive at room temperature (λ_{max} = 565 nm) with quantum yield of 0.025.

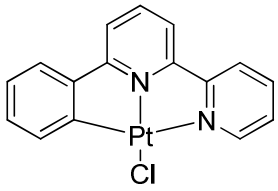

Pt(C^N^N)Cl

Figure 3: An example of a Pt(C^N^N) complex

Pt(C^N^C) Complex

This complex can be prepared using the 2,6-diphenylpyridine ligand. This ligand contains two phenyl groups on the outer portions of the ligand. The platinum complex that uses this ligand is emissive at 568nm at room temperature in its solid state, as shown in **Figure 4**.[17]

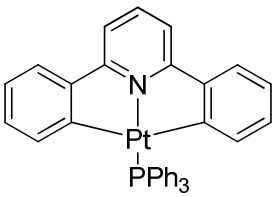

Pt(C^N^C)PPh_3

Figure 4: An example of a Pt(C^N^C) complex

Pt(N^C^N) Complex

This complex can be prepared by using the ligand 3-di(2-pyridyl)benzene (dpybH).[18] In this ligand, the phenyl ring occupies the central position in the ligand. The platinum complex

that is prepared using this ligand, as shown in **Figure 5,** is emissive at room temperature with λ_{max}= 496 nm.

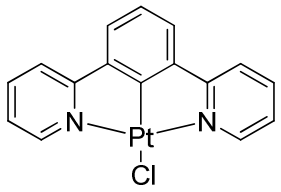

Pt(N^C^N)Cl

Figure 5: An example of a Pt(N^C^N) complex

*Pt(C^N*N) Complex*

A new class of tridentate complexes that has been developed has shown promising photophysical properties. These complexes contain a fused five-six-membered metallacycle (**Figure 6**); whereas the previous three tridentate complexes have a fused five-five-membered metallacycle. The coordination of this new class of tridentate complex allows for a geometry that is closer to a square planar geometry, which has shown an improvement in the quantum yield. The quantum yield of the complex in **Figure 6** was measured to be 56% while the similar complex with the five-five-membered metallacycle has only a 4% quantum yield at room temperature.[19]

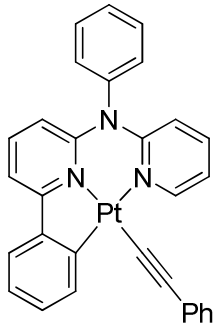

Figure 6: (C^N*N)PtCCPh complex

These classes of cyclometalated platinum complexes have been broadly investigated in the past. In recent years, more interest has been given to the tridentate cyclometalated complexes, especially those derived from the C^N^N (6-phenyl-2,2'-bipyridine), C^N^C (2,6-diphenylpyridine), and N^C^N (1,3-dipyridylbenzene) ligands discussed above and illustrated in **Figures 3**, **4**, and **5**.[20]

Tetradentate Complexes

It has been observed that rigidity favors luminescence, which makes tetradentate bis-cyclometalated complexes a promising class of platinum complexes. They can be represented by their coordination pattern of the ligand such as (C^N^N^C) Pt complex[21] as shown in **Figure 7**. A novel complex of this coordination has been reported with a high quantum yield. The complex emits intensely in solution at room temperature with quantum yields of 0.74 and λ_{max}= 512 nm. This complex is thermally stable and when fabricated for OLED, it exhibited 13% external quantum efficiency.

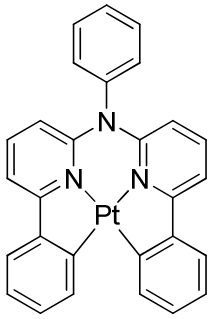

Figure 7: Tetradentate platinum complex with C^N*N^C coordination

Square-planar cyclometalated platinum(II) complexes have received much attention over the last two decades due to their intrinsic photophysical properties.[22] The introduction of a strong carbon σ donor, like a C-Pt bond, into a complex can allow for a considerable influence on the excited state of the complex. This can be seen when a carbon σ donor induces a switch from a non-radiative d-d transition to a metal to ligand charge transfer (MLCT), a ligand centered (LC) transition, or a mixture of both, depending on the nature of the ligands, due to the large d orbital splitting caused by the strong ligand effect of the carbon donor making the unoccupied dx^2-y^2 orbital inaccessible for electron transitions, as shown in **Figure 8**. Some things to note about this figure (**Figure 8**) are that the relative energy levels of the d orbitals may vary depending on the nature of the various ligands, however, the dx^2-y^2 orbital always has the highest energy. The simplified energy diagram also does not take into account the interaction between the metal and the ligand orbitals. This switch in charge transfers promotes the intense phosphorescent emission when the contribution from the platinum atom is involved in the excited states (typically a contribution to the HOMO of the complex). This is made possible by the strong spin-orbital coupling induced by platinum, which has a high spin-orbital coupling

constant. This effect will promote the intersystem crossing, which is an isoenergetic radiationless transition, from the singlet state to the triplet state making phosphorescent emission possible (see **Figure 9**). On the other hand, fluorescence emission is limited to the radiative relaxation of the electrons in an organic molecule where the spin is conserved. These energy states mentioned refer to the pairing of electrons. A singlet state is the molecular orbital state where the electron spins are paired, whereas a triplet state contains electron spins that are unpaired.

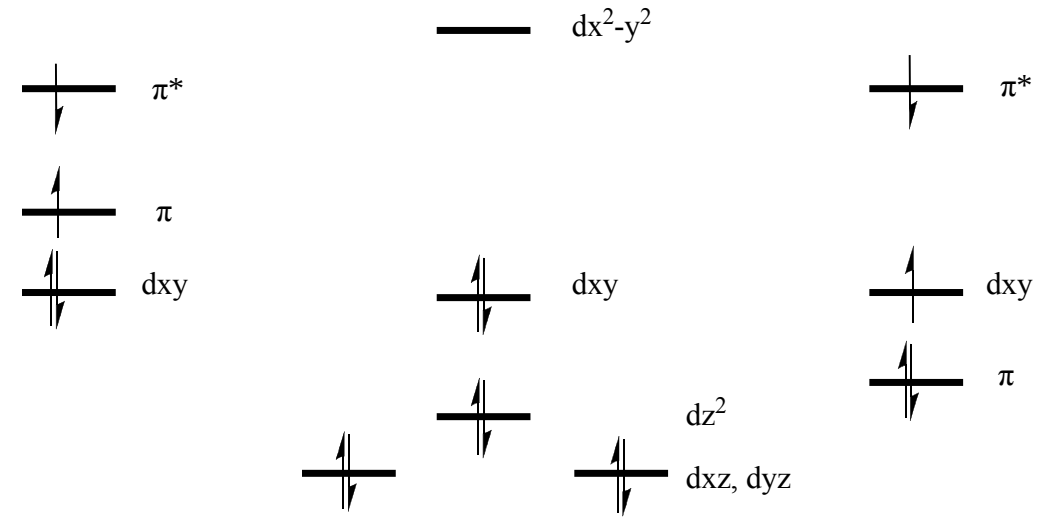

Ligand-centered state **Ligand field-splitting of metal d orbital in square-planar d^8 metal complex** **MLCT state**

Figure 8: Simplified ligand and metal orbital energy diagram for MLCT and LC states

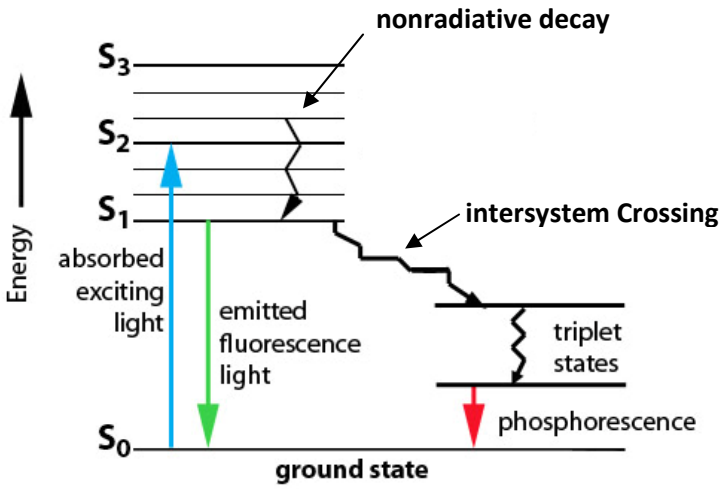

Figure 9: Schematic decay pathway of fluorescence and phosphorescence

The strong phosphorescent emission, especially at room temperature, exhibited by cyclometalated platinum complexes has paved the way for the use of these complexes in a wide range of applications. Some of these applications are optical chemosensors[23], photocatalysts[24], solar cells[25], biological labels[26], and electroluminescent emitters in organic light emitting diodes (OLEDs).[27,28,29,30,31] One of the most recently investigated applications of cyclometalated platinum complexes has been the photogeneration of hydrogen from water.[32]

Even though there has been much progress made in the past two decades, there is still a large demand for new materials with certain photophysical and electrochemical properties that are stable under the conditions required for their use in various applications. There are many examples illustrating this fact, especially with the need for greater stability in photo-oxidation, which uses platinum complexes as sensitizers, which can be practically used in photosensitized oxidation reactions with solar energy and air. There have also been many advances in the

application of phosphorescent emitters in OLED devices; however, the efficiency or stability or both associated with the cyclometalated platinum complexes are still issues that need to be improved.

In an effort to improve upon some of these issues, the Huo research lab designed a variety of tetradentate cyclometalated platinum complexes with different coordinations in order to study their photophysical properties.[33] However, when the ligand was put through a complexation reaction, **Scheme 1**, and characterized, some surprising results were obtained. It was found that after allowing the ligand to react with K_2PtCl_4 in glacial acetic acid, AcOH, the sp^3 C-H bond of the butyl group was activated as opposed to the desired sp^2 C-H bonds on the phenyl groups.[34] After establishing that sp^3 C-H bond activation takes place in this type of reaction, our lab began to study the selectivity of the reaction during cycloplatination.

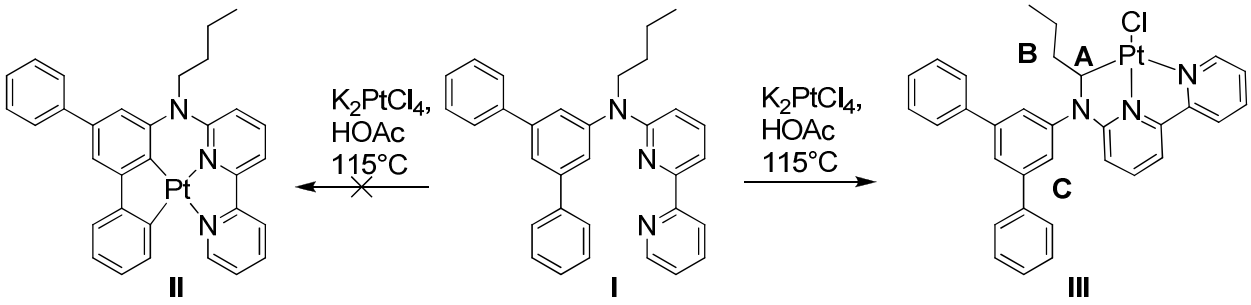

Scheme 1: Complexation of ligand **I**

In transition metal complexes, it is generally recognized that an aromatic C-H bond is more reactive toward activation. For this reason, it was assumed the reaction in **Scheme 1** would have proceeded to complex **II**. However, a study published in 2009 states that a delicate balance

between sp^2 and sp^3 C-H bond activations exists in the platinum (II) complex.[35] After searching to determine what is known about the selectivity of cycloplatination, it was found that the mechanism of cyclometalation is not fully understood. Other papers attempt to explain the stability of sp^2 and sp^3 substituted complexes, as well as the formation of five-membered and six-membered metallacycles. Zucca's paper discusses this topic by studying the stability of rhodium complexes, one that contains a six-membered ring due to a sp^2 substitution, while the other has a five-membered ring due to the substitution on a sp^3 carbon, as shown in **Figure 10**.[36] However, there is no explanation given for the selectivity of the reaction.

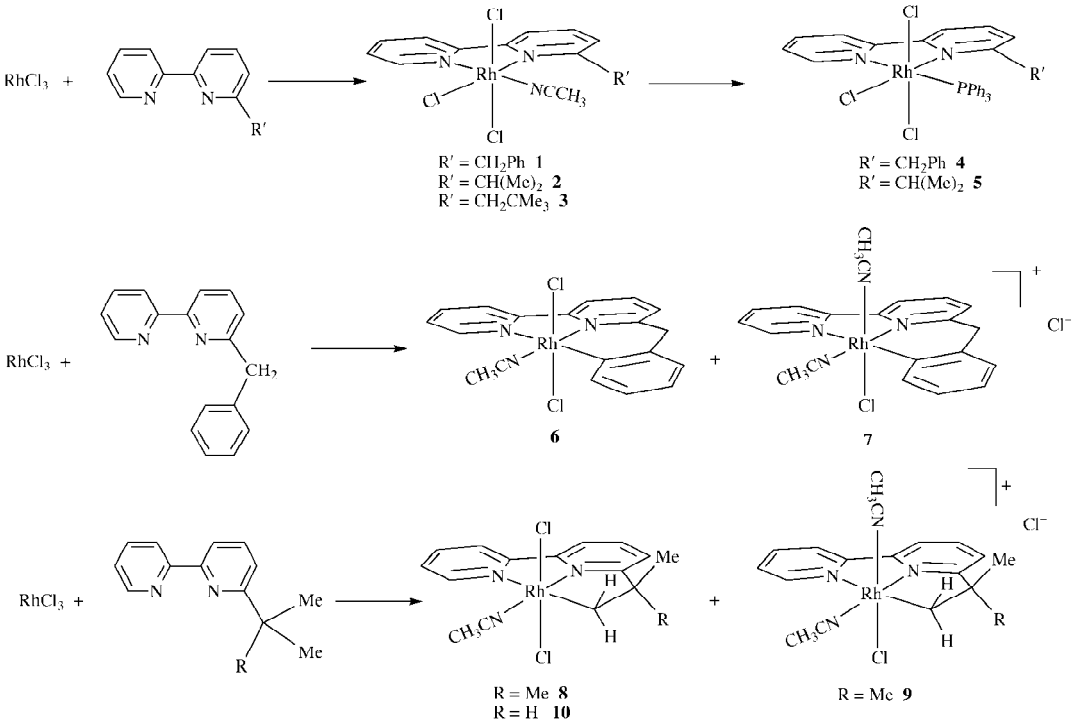

Figure 10: Stability of sp^2 vs. sp^3 and five-membered ring formation vs. six-membered ring formation

C-H bonds are ever-present in organic molecules, but the vast majority of them cannot be exploited for chemical reactions due to their inert and stable nature. Early attempts to activate these bonds led to very complicated mixtures of products, and therefore not an acceptable means of C-H activation.[33] Organic molecules that contain carbon chains make up a large portion of the non-metallic materials frequently used in everyday life, like plastics. The difficulty in the manufacturing of plastics is that they are a product of the chemical synthesis from hydrocarbons found in petroleum. Only a few of the hydrocarbons found in petroleum are reactive enough to undergo traditional chemical reactions.[33] In order to make the synthesis of non-metallic materials more efficient, C-H activation was needed to stimulate these inert hydrocarbons to make them more reactive.

Interest in this area of chemistry began in the 1980's when there was a dramatic increase in the number of metal salts and complexes that were found to initiate C-H bond activation by the process of oxidative addition. A drawback to this form of C-H activation was that most of these transformations required equal amounts, in moles, of the hydrocarbon and the metal, which would both be consumed during the reaction. This is not acceptable for large-scale chemical applications, as the metals involved as the starting material and intermediates are generally more expensive than the products.[37] In recent years there has been an explosion of interest in using catalysts to promote the oxidative addition needed to activate C-H bonds. In these catalytic processes, "the oxidative addition product is a transient intermediate that immediately reacts with other reagents to introduce a new atom,"[33] into the ligand. After performing this addition, the catalytic metal is released so that it is able to attack another molecule of hydrocarbon. This allows for the normally expensive catalyst to be used in very small amounts.

There has been much debate over the C-H bond cleavage mechanism since Shilov and his coworkers reported on the activation of alkanes by solutions of platinum (II) chlorides.[38] It is still unclear as to which mechanism drives the reaction. There are several examples summarized in one journal article by Ryabov that states "sometimes platinum (II) displays electrophilic features, for example, on cyclometalation of azobenzene[39] and N,N-dimethylbenzylamine,[40] but sometimes it reacts via oxidative addition…mechanistic information on cycloplatination can be found in a family of kinetic investigations of mechanisms of reactions by platinum (II)" [41] as well.

Cycloplatination via sp^3 C-H activation is known and has been reported in a few articles. In an article by Zucca,[42] it is stated that, in general, nitrogen donor ligands tend to form five-membered rings, but there are a few six-membered rings that have been uncovered. The article goes on to say that the majority of the papers published in this field discuss the C(sp^2)-H bond activation, and that only a few cyclometallated species that contain nitrogen ligands and C(sp^3)-Pt bonds are known while only two six-membered cyclometallated species with a Pt-C(sp^3) bond have been reported.[43] Zucca uses the ligands shown in **Figure 11** to test the selectivity of platination. **Figure 12** shows the location of cycloplatination after reaction with K_2PtCl_4.

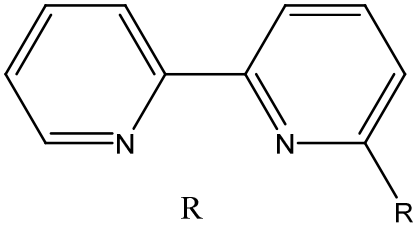

Figure 11: Ligands tested for their selectivity of cycloplatination

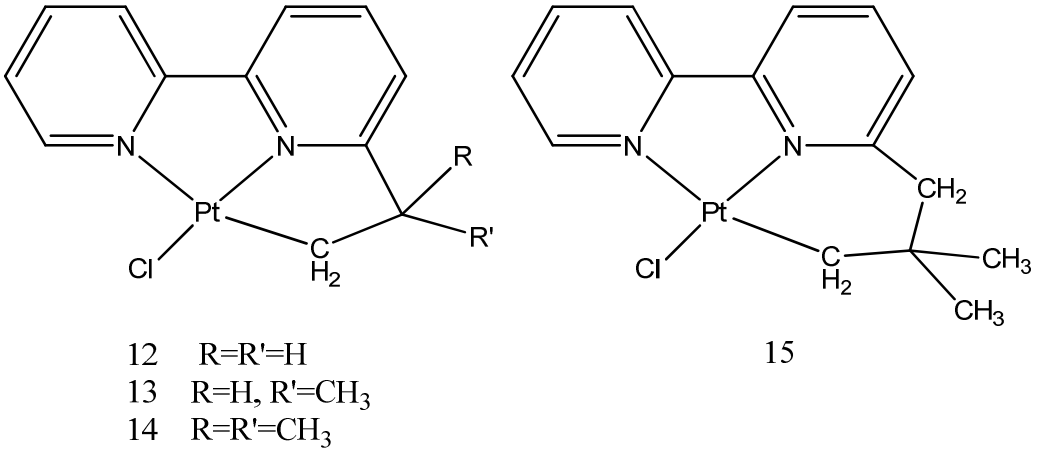

Figure 12: Location of cycloplatination for reported ligands

There has also been some research performed on the selectivity of reactions by taking into account theoretical considerations that can unveil underlying structure-reactivity relationships.[44] These studies are important to examine the stability of possible intermediates and transition states. In one published work by Marrone et al.[45] a proposed pathway of cyclometallation of a ligand is shown in **Figure 13** while density functional theoretical (DFT) calculations are used to illustrate the plausibility of this pathway in **Figure 14**.

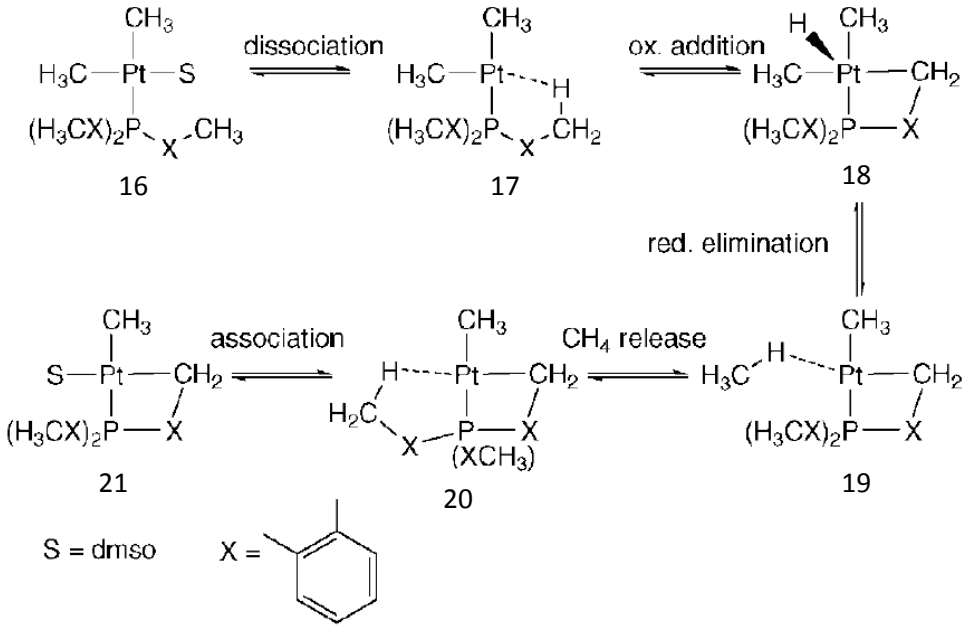

Figure 13: Reaction pathway proposed for cyclometalation of 16

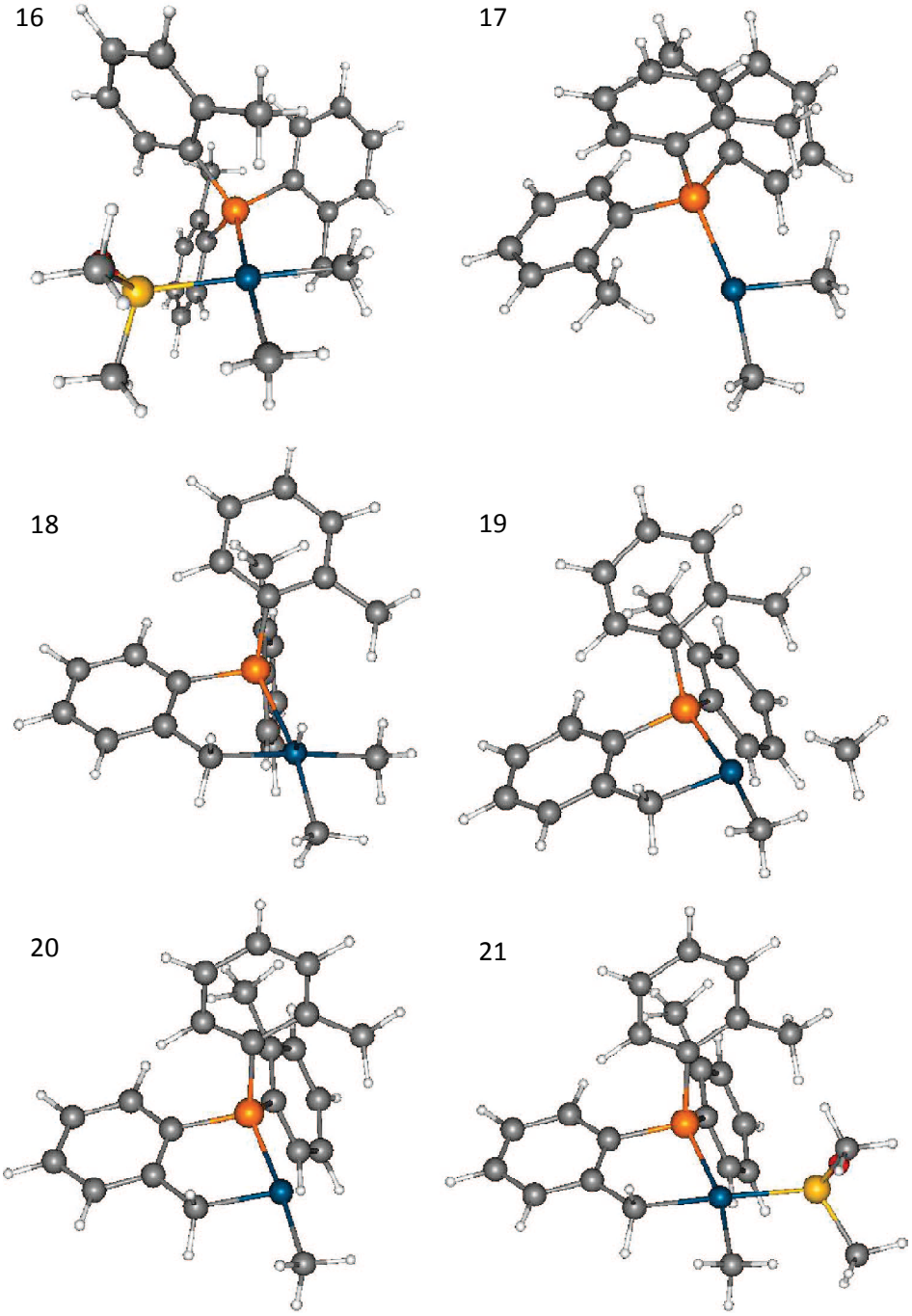

Figure 14: DFT optimized geometries of complexes 16-21

In the initial days of this project, when the selectivity of cycloplatination was being studied, it was observed that one of the ligands designed to test whether sp^2 or sp^3 substitution would predominate, or if ring size was a factor, not only produced one of the desired products when reacted with K_2PtCl_4 in AcOH, but also produced some side products that formed from an interaction with the solvent. To avoid this issue, another solvent was chosen for the reaction. When the product from this reaction was characterized, it was found to be an isomer of the first product that was formed in AcOH. This reaction, along with the side products, will be discussed in much more detail in the following sections.

It was found that studies of solvent-manipulated control over the selectivity of C-H bond activation are rarely seen. One of the few exceptions was that of an *ortho*-palladation of *N*-thiobenzoylpyrrolidine reported by Yoshida in 1981,[45] where the cyclometalation occurred at either the phenyl ring or the pyrrolidine ring depending on the solvent used for the reaction (**Scheme 2**); however, no explanation was given for this switch in the selectivity. Needless to say, this developed a great interest in the solvent-controlled switch of selectivity by platinum (II) metal, and led to the goals of this research project.

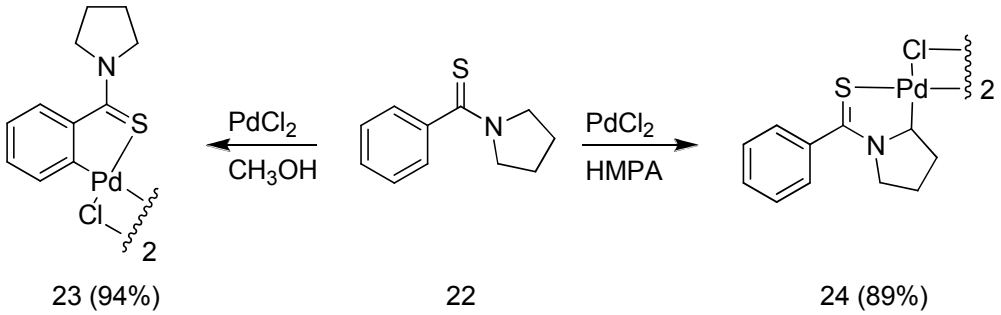

23 (94%) 22 24 (89%)

Scheme 2: Switch of selectivity using different solvents

CHAPTER 2: RESEARCH GOALS

As stated in chapter 1, this research came to fruition from an earlier project in the research lab where ligand **I** was originally designed to be a tetradentate complex with a N^N*C^C coordination pattern. However, the platinum atom selectively bound to carbon A. The question that must be answered is why did the cycloplatination not occur on either carbon C or even carbon B (**Figure 15**)?

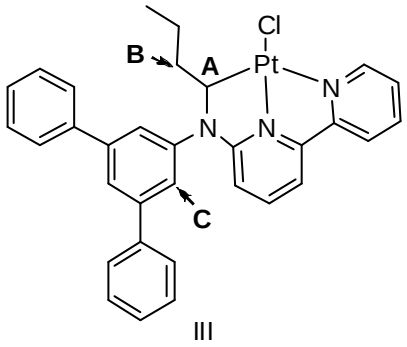

III

Figure 15: Complex **III** after reacting **I** with K_2PtCl_4 in AcOH

After discovering this product from the reaction, it was deemed important to determine the selectivity of cycloplatination of certain ligands. Selectivity in chemical reactions is a very important factor when designing and synthesizing compounds. To understand the underlying factors that are responsible for this selectivity is even more important and is therefore a goal for this research. To do this, several ligands were synthesized and their complexation with K_2PtCl_4 was examined.

The tridentate ligands allows for the study of several issues involved in the cycloplatination through the use of careful ligand design. The ligands shown below (**Figure 16**)

will help to examine the following issues: (1) relative reactivity of sp^2 C-H and sp^3 C-H (**L1-L4**), (2) the competition between five and six-membered ring formations (**L1**, **L2** and **L3**).

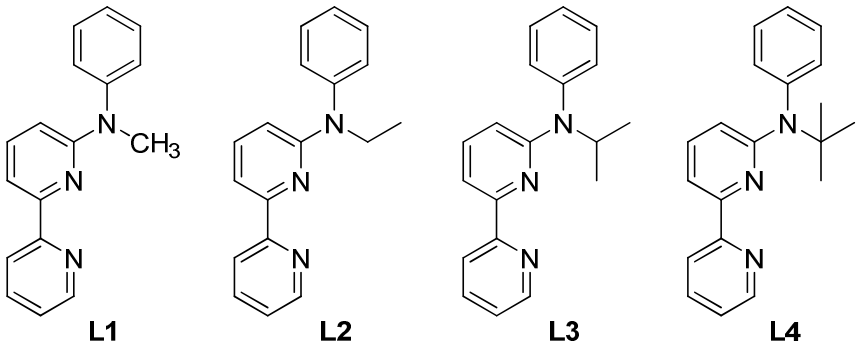

Figure 16: Ligands designed to test the selectivity of cycloplatination

Cycloplatination of **L1** can determine whether platinum will bind to the sp^3 carbon of the methyl group or the sp^2 carbon of the phenyl ring. If it binds to the methyl carbon there will be a five-membered ring and a six-membered ring if it binds to the phenyl's carbon. This ligand has two variables to test, sp^2 versus sp^3 C-H bond activation as well as five and six membered ring formation. **L2** and **L3** have the potential to determine whether ring size or reactivity of the carbons, a sp^2 versus a sp^3 carbon, influences the selectivity of cycloplatination better. **L4** will be used to study only the sp^2 versus sp^3 reactivity aspect as the ring size will be the same at either probable location of cycloplatination.

As was mentioned in Chapter 1, this research was also carried out to study the solvent controlled switch of selectivity between sp^2 and sp^3 C-H bond activation using platinum (II). Initially, all of the complexation reactions were run using glacial acetic acid, AcOH, as the solvent. The use of a different solvent came about as the products of the cycloplatination

reaction of **L3** were isolated and characterized. The major product was one of the expected isomers, while the other two products came about due to side reactions from the C-N bond cleavage as well as an interaction with the solvent. In order to circumvent these side products from forming, a different solvent was chosen to run the reaction in. The solvent chosen for this reaction was acetonitrile, CH_3CN, and after characterizing the major product from the reaction in this solvent, it was determined that one of the other possible isomers was the major product. After running this reaction, it was determined that it was necessary to repeat all the complexation reactions of the other ligands in acetonitrile and to characterize the products in order to observe the selectivity of the reactions.

In order to characterize the structure of these complexes after synthesis, a variety of instruments and techniques were used. Mass spectrometry was used to obtain the molecular weight. Gas chromatography-mass spectrometry (GC-MS) was used for the intermediates, while a mass spectrometer, equipped with Q-TOF detector, operated in ESI mode was used to obtain the molecular weight of the complexes. 500 MHz nuclear magnetic resonance (NMR) was also used to obtain high resolution proton spectra to determine the splitting pattern in the aromatic region. This can illustrate the disappearance of protons in the complex spectra, when compared to the ligand spectra, which is indicative of complexation. The 300 MHz NMR was used to obtain ^{13}C spectra of the ligands and complexes. Another tool that was used in characterization was X-ray crystallography, which elucidates the geometrical conformation of the complexes, such as planarity, bond lengths, and angles around the platinum coordination center. Elemental analysis was also of use in determining the composition of the synthesized complexes.

After characterization, the focus then shifted to the underlying factors responsible for this interesting selectivity in the intramolecular C-H bond activation. For these studies, the thermodynamic and kinetic controls of the reactions in different solvents were examined. The last study to be undertaken involved the side reactions of **L2**, **L3** and **L4** which will be discussed in chapter 5.

CHAPTER 3: SOLVENT CONTROLLED SWITCH OF SELECTIVITY DURING CYCLOPLATINATION REACTIONS

The previous chapters have shown some important properties of platinum complexes as well as some strategies that can be exploited in the design of platinum complexes. This chapter deals with the characterization of tridentate platinum complexes that contain the various substituents that were discussed in the previous chapter as a means to test the selectivity of cycloplatination when the solvent is switched. Techniques such as NMR, mass spectrometry and X-ray crystallography were used for the characterization of the synthesized complexes. The ligand and complexation schemes will be shown, as will comparisons of the ligand and complex NMR spectra to determine where the selectivity of the reaction took place, and X-ray crystal structures for some of the complexes. Just the reaction scheme for each reaction will be given in this chapter, the reaction conditions can be found in the experimental chapter.

Complexation of the Methyl Ligand (L1) in AcOH

*Synthesis of N-methyl-N-phenyl-2,2'-bipyridin-6-amine (**L1**)*

The methyl substituted ligand, **L1**, was synthesized using the procedure shown below in **Scheme 3**, where the pure product was isolated with a 79% yield.

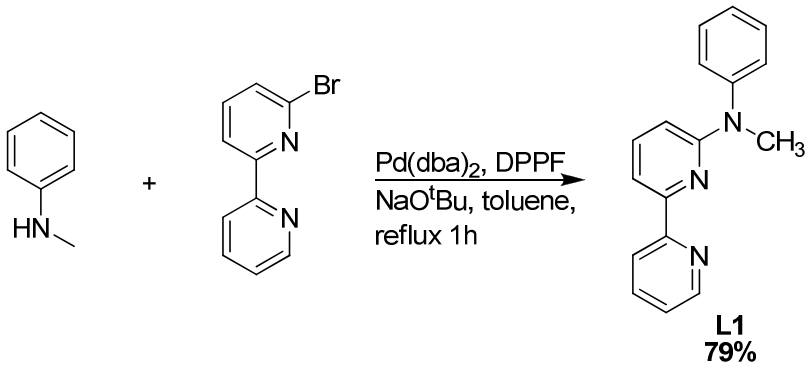

Scheme 3: Synthesis of *N*-methyl-*N*-phenyl-2,2'-bipyridin-6-amine

*Complexation of **L1** in AcOH*

After the ligand was synthesized, it was then complexed with potassium tetrachloroplatinate (K_2PtCl_4) in AcOH (**Scheme 4**). **Scheme 4** illustrates the two possible isomers from this reaction. After characterization, it was found that the major product was that of **1A** with a 73% yield after purification. The isomer was able to be characterized by comparing the NMR spectra of both **L1** and the purified product (**1A**) from this reaction (**Figure 17**).

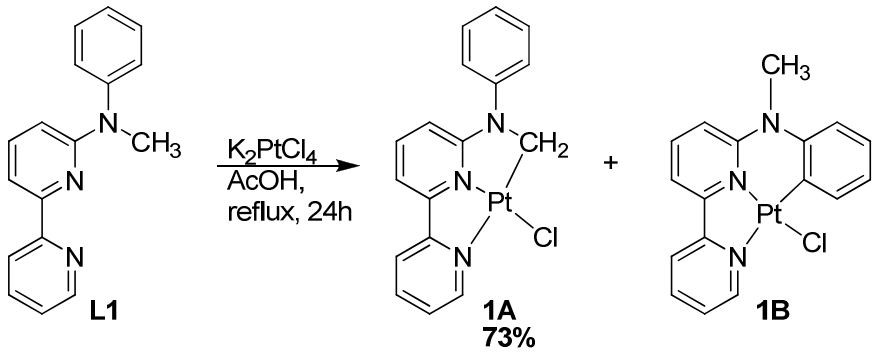

Scheme 4: Possible isomers of the complexation of **L1** in AcOH

The peak for the protons of the methyl group for the ligand is found at 3.61 ppm and is a singlet. The peak for the same protons for the complex has been shifted downfield to 5.55 ppm and again is a singlet; however, there are two small peaks on either side of the singlet called satellite peaks that occur due to the platinum's coupling of the hydrogens in the methyl group. These satellite peaks have a $^{2}J_{Pt\text{-}H}$ coupling constant of 40.5 Hz. **Figure 18** showes an expanded view of this peak showing the satellite peaks. Also, the peak from the ligand's methyl group protons has completely disappeared. The aromatic region of these spectra also gives a good indication that complexation has occurred as they are distinctly different when studying the

distribution of the peaks from the aromatic protons. After integration of all the peaks, it was found that there are 14 hydrogens in the complex's spectra, whereas there are 15 in the ligand's spectra, showing that cycloplatination has occurred (integration was performed by defining the aromatic proton peak at 6.5 ppm as one hydrogen).

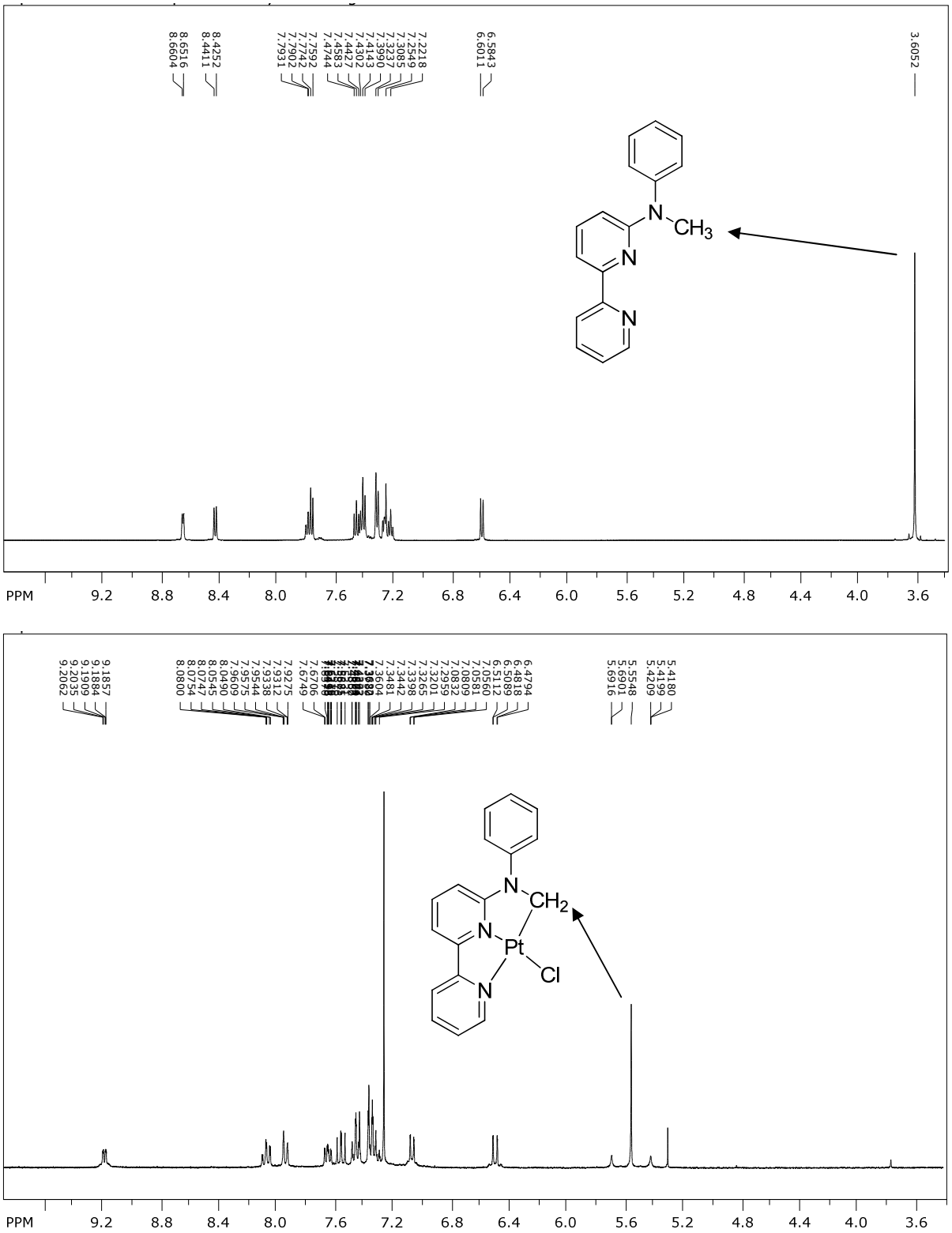

Figure 17: Comparison of **L1**'s (top) and complex **1A**'s (bottom) NMR spectra

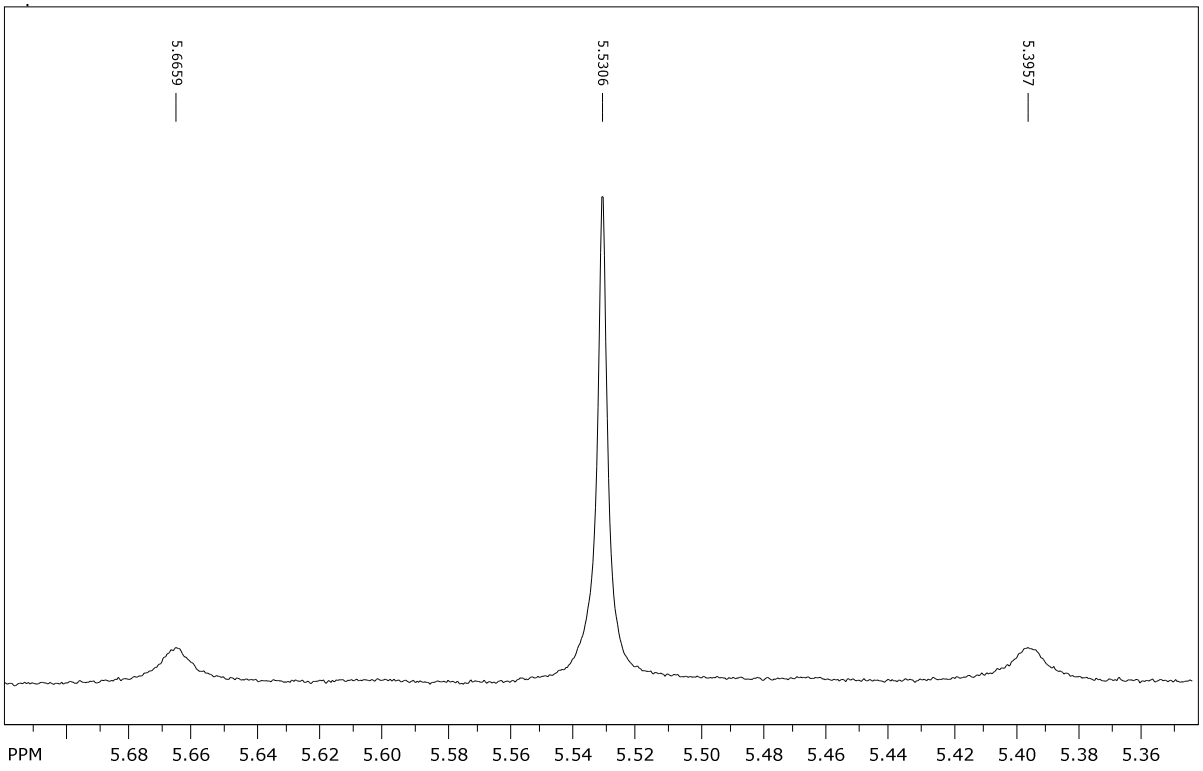

Figure 18: Satellite peak from NMR spectrum of complex **1A**

From these NMRs, it was possible to identify the product of the complexation reaction of **L1** in AcOH as being the sp^3 substituted product, where the C-H bond in the methyl group was activated by the platinum metal. The crude reaction mixture was also examined using NMR to determine the ratio of sp^3 to sp^2 product formation. It was found that the ratio of sp^3 to sp^2 from this reaction was 96:4.

Complexation of the Ethyl Ligand (L2) in AcOH

*Synthesis of N-ethyl-N-phenyl-2,2'-bipyridin-6-amine (**L2**)*

The ethyl substituted ligand, **L2**, was synthesized using the procedure shown below in **Scheme 5**, where the pure product was isolated with an 89% yield.

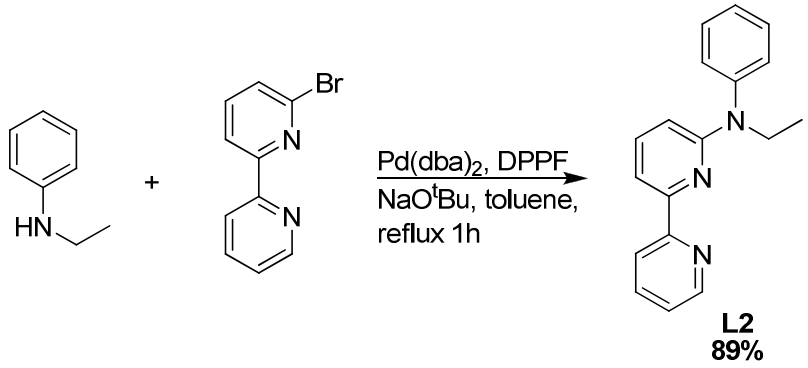

Scheme 5: Synthesis of *N*-ethyl-*N*-phenyl-2,2'-bipyridin-6-amine

*Complexation of **L2** in AcOH*

After the ligand was synthesized, it was then complexed with potassium tetrachloroplatinate (K_2PtCl_4) in AcOH (**Scheme 6**). **Scheme 6** illustrates the three possible isomers from this reaction. After characterization, it was found that the major product was that of **2A** with a 63% yield after purification. The isomer was able to be characterized by comparing the NMR spectra of both **L2** and the purified product (**2A**) from this reaction (**Figure 19**).

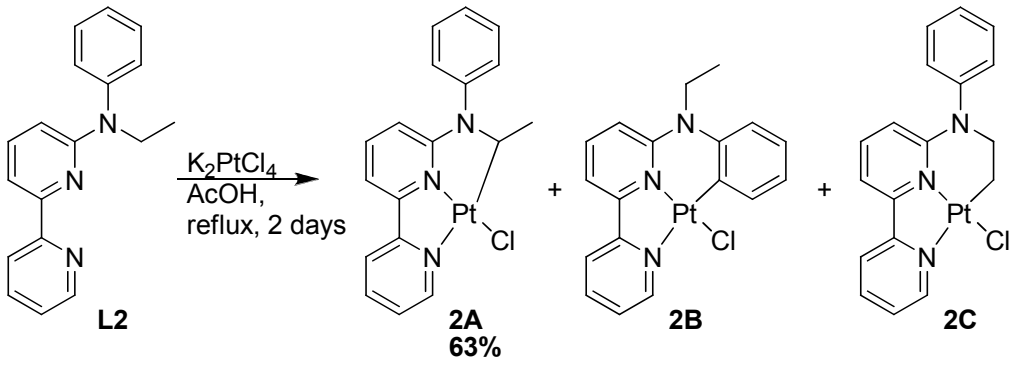

Scheme 6: Possible isomers of the complexation of **L2** in AcOH

The peak for the protons of the methyl group in the ligand shows up at 1.31 ppm and splits into a triplet, while the peak for the primary carbons's protons shows up at 4.15 ppm and splits to form a quartet. The peak for the protons of the methyl group in the complex have shifted downfield slightly to 1.40 ppm and has a doublet for its multiplicity. This peak also has satellite peaks with a $^{3}J_{\text{Pt-H}}$ coupling constant of 21.5 Hz. The peak for the protons of the secondary carbon has been shifted downfield to 5.88 ppm and splits into a quartet. This peak also has satellite peaks with a $^{2}J_{\text{Pt-C}}$ coupling constant of 48.0 Hz. F**igure 20** is an expanded view of these peaks showing the satellite peaks. Integration was also used to determine that cycloplatination occurred.

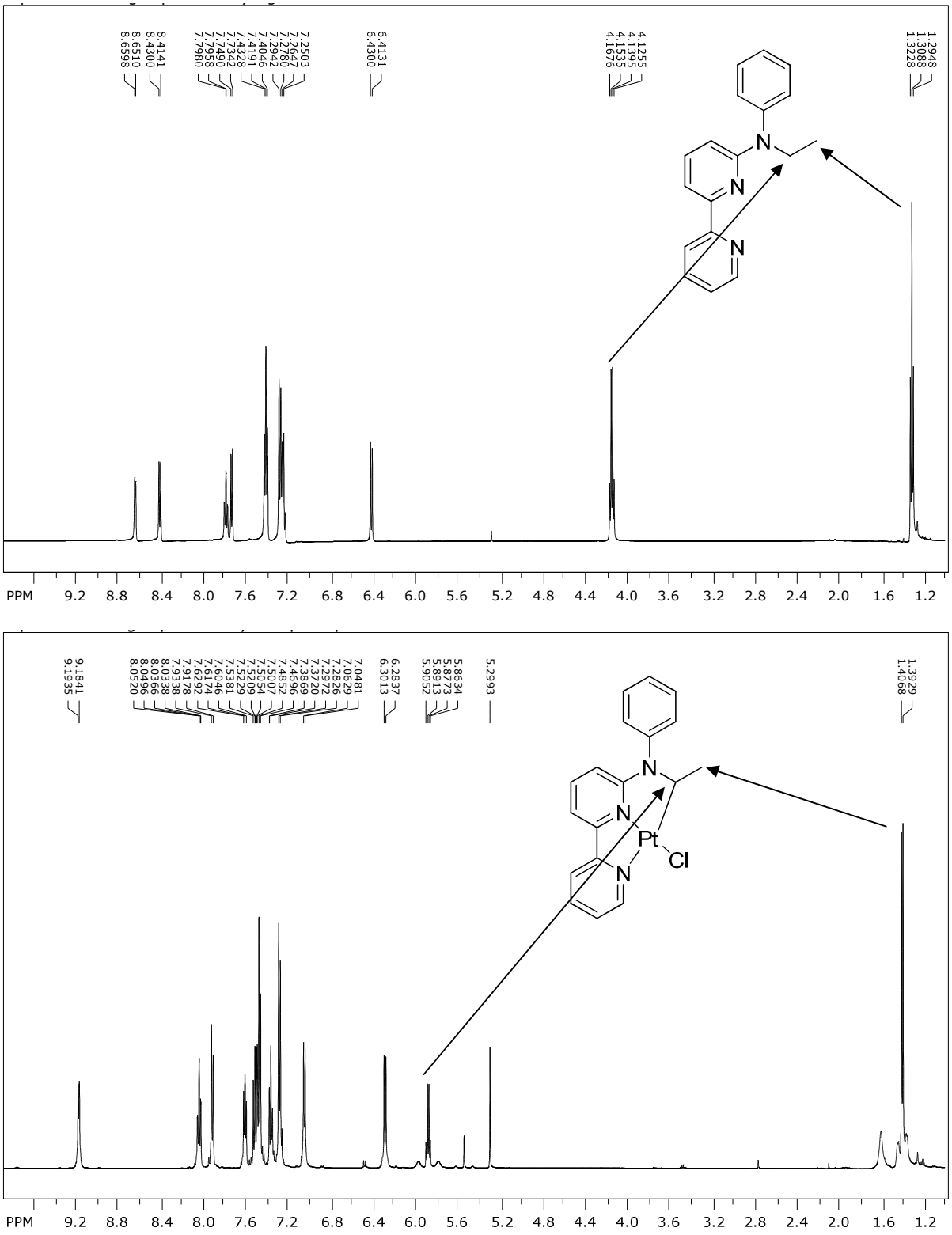

Figure 19: Comparison of **L2**'s (top) and complex **2A**'s (bottom) NMR spectra

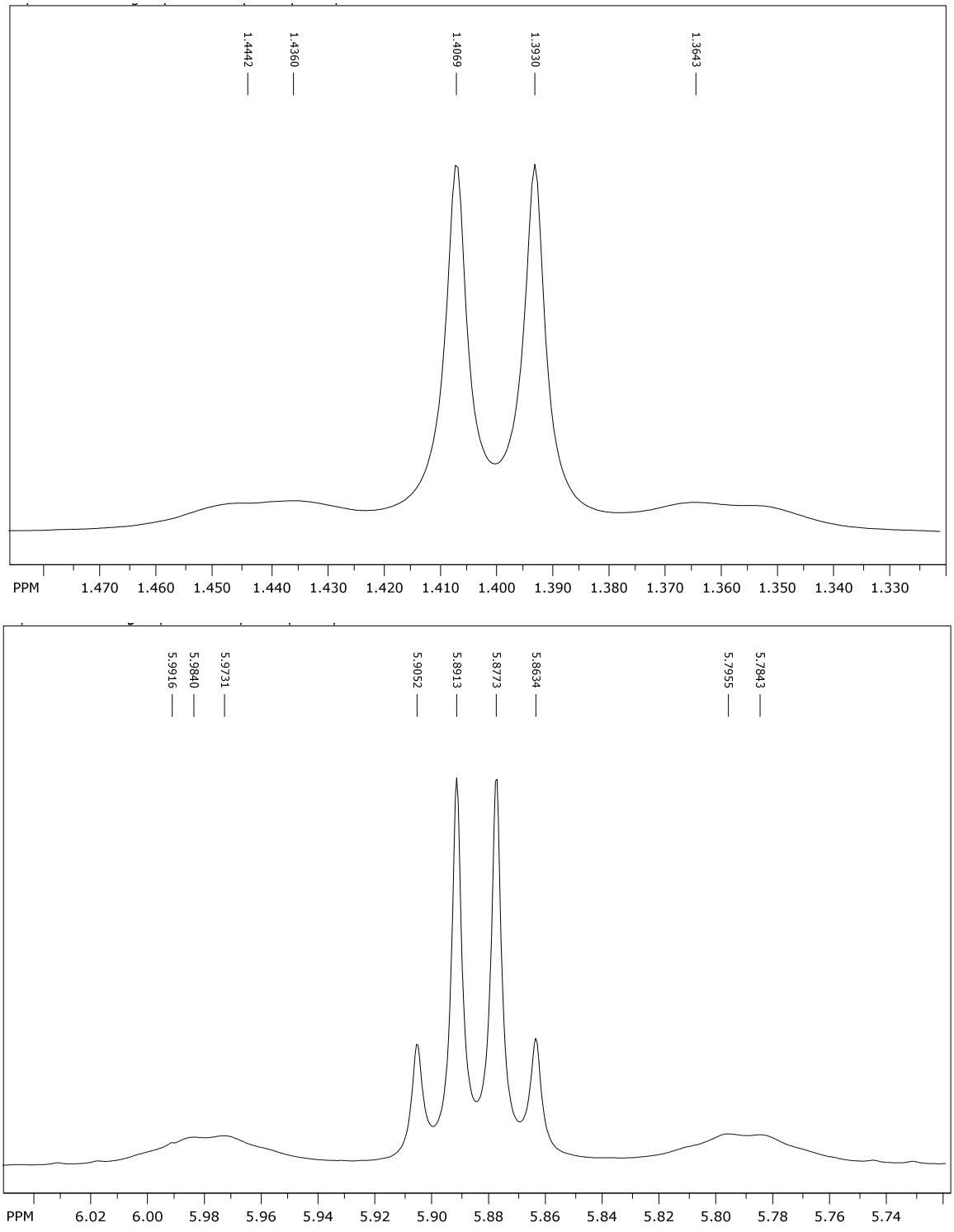

Figure 20: Satellite peaks from NMR spectra of complex **2A**, methyl protons (top), primary protons (bottom)

It is evident that the cycloplatination occurred for this complexation reaction since the primary carbon lost one of its two hydrogens which made the peak belonging to the protons of the methyl group to go from a triplet to a doublet. The aromatic region is also noticeably different in the distribution of the aromatic protons. When examining the integration of the peaks it is evident that cycloplatination has occurred due to the loss of a hydrogen. There are 17 hydrogens in the ligand and only 16 hydrogens in the complex (integration was performed by defining the aromatic proton peak at 6.3 ppm as one hydrogen). The crude reaction mixture was also examined using NMR to determine the ratio of sp^3 to sp^2 product formation. It was found that the ratio of sp^3 to sp^2 from this reaction was 97:3, it should also be stated that there was no formation of complex **2C**.

Complexation of the Isopropyl Ligand (L3) in AcOH

*Synthesis of N-isopropyl-N-phenyl-2,2'-bipyridin-6-amine (**L3**)*

The isopropyl substituted ligand, **L3**, was synthesized using the procedure shown below in **Scheme 7**, where the pure product was isolated with a 55% yield.

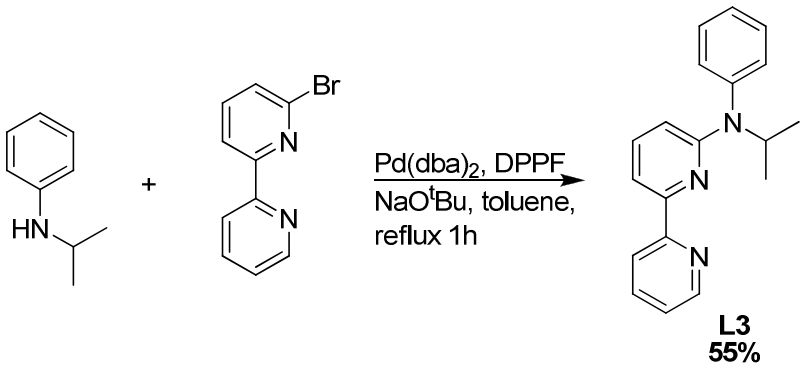

Scheme 7: Synthesis of *N*-isopropyl-*N*-phenyl-2,2'-bipyridin-6-amine

*Complexation of **L3** in AcOH*

After the ligand was synthesized, it was then complexed with potassium tetrachloroplatinate (K_2PtCl_4) in AcOH (**Scheme 8**). **Scheme 8** illustrates the three possible isomers from this reaction. After characterization, it was found that the major product was that of **3A** with a 38% yield after purification. The isomer was able to be characterized by comparing the NMR spectra of both **L3** and the purified product (**3A**) from this reaction (**Figure 21**).

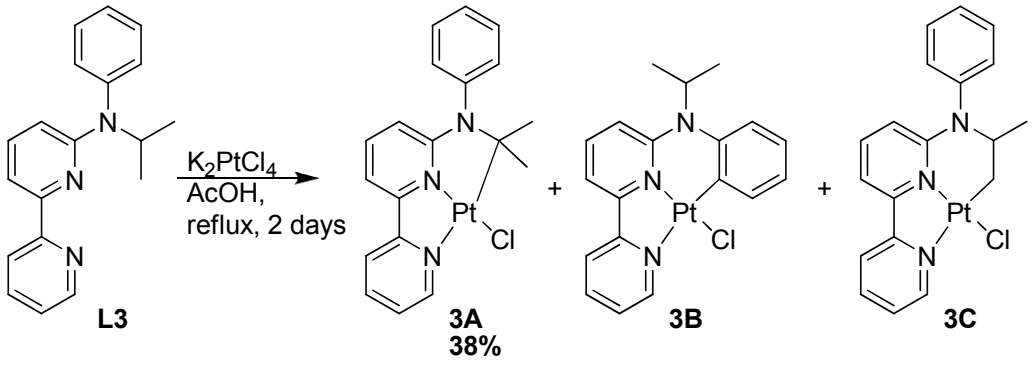

Scheme 8: Possible isomers of the complexation of **L3** in AcOH

The peak for the protons of the methyl groups in the ligand shows up at 1.22 ppm and splits into a doublet, while the peak for the secondary carbons's protons shows up at 5.42 ppm and splits to form a septet. The peak for the protons of the methyl groups of the complex have shifted downfield to 1.48 ppm and has a singlet for its multiplicity. This peak also has satellite peaks with a $^{3}J_{Pt\text{-}H}$ coupling constant of 17.5 Hz, **Figure 22** is another expanded view of this

peak with its satellite peak. The peak for the proton of the secondary carbon has disappeared due to the platinum binding to this location.

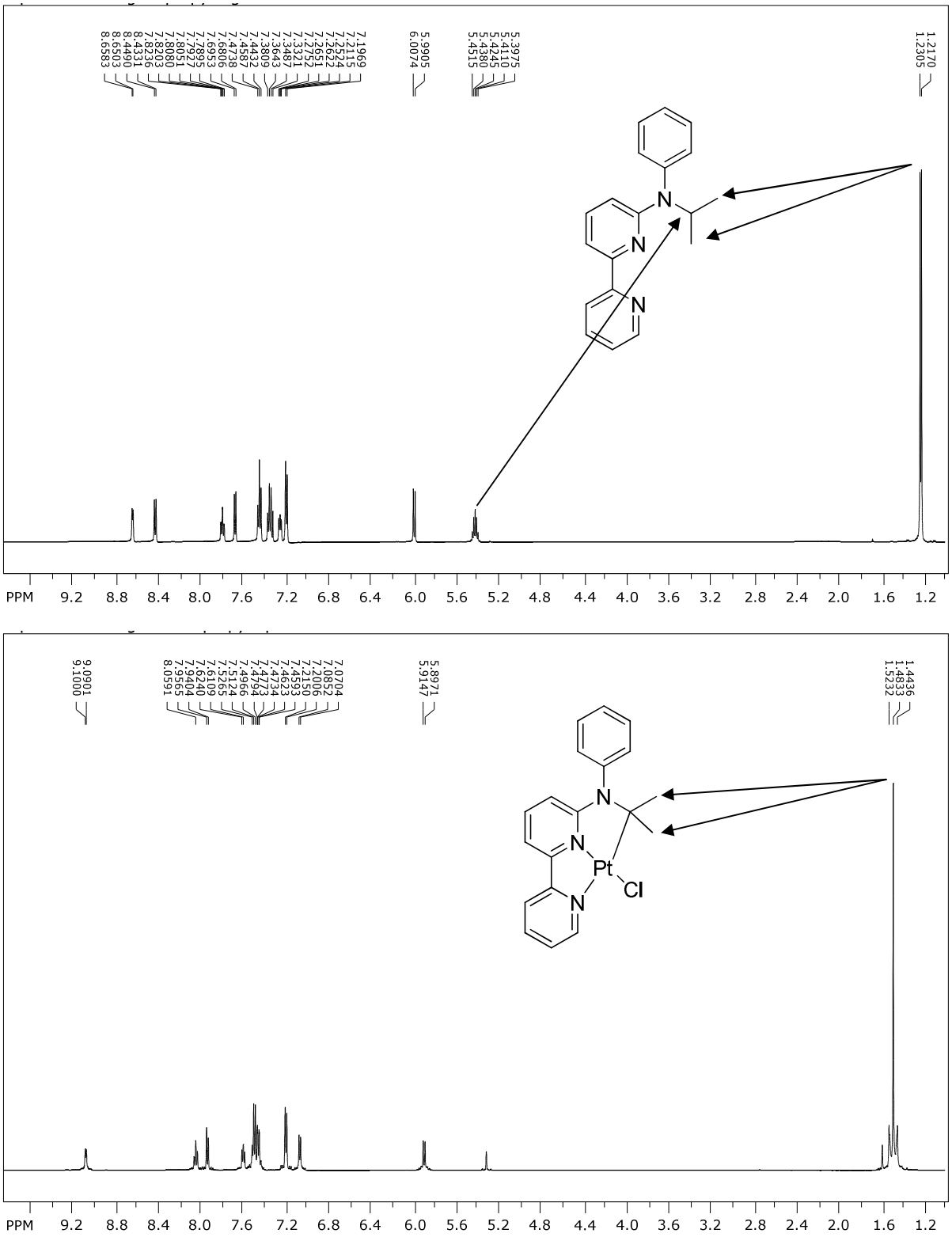

Figure 21: Comparison of **L3**'s (top) and complex **3A**'s (bottom) NMR spectra

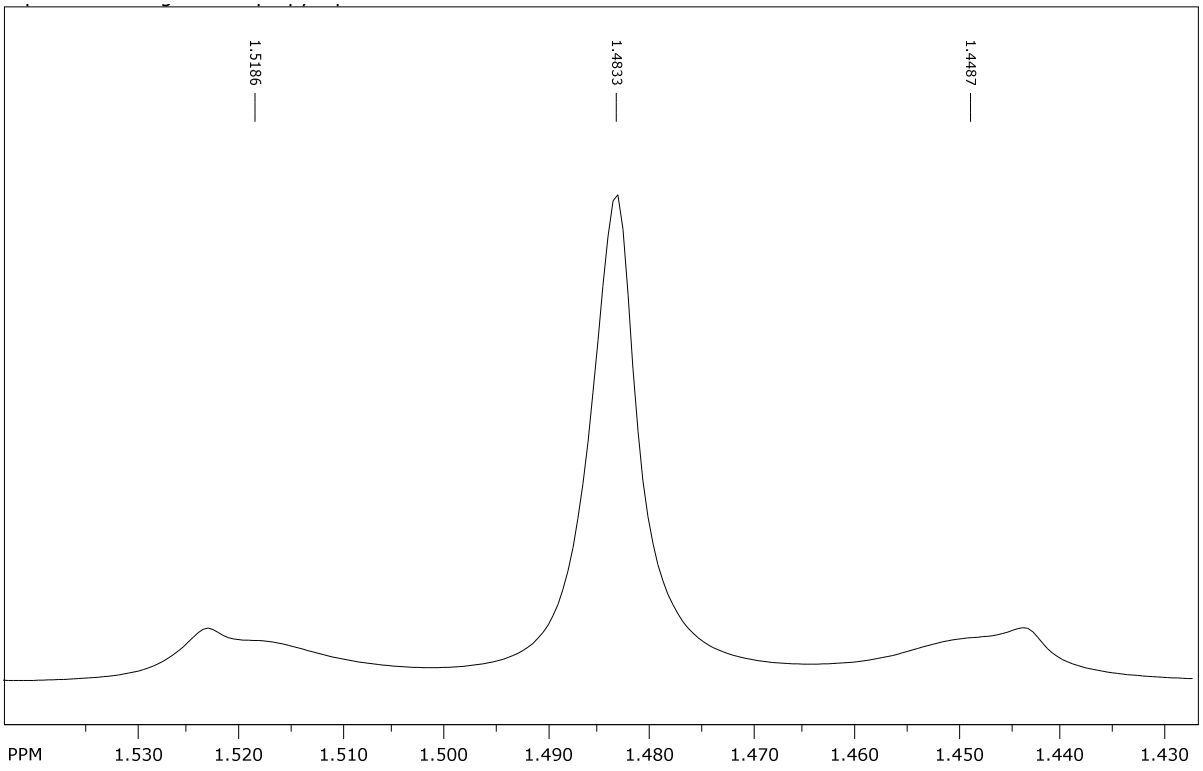

Figure 22: Satellite peaks from NMR spectra of complex **3A**

It is evident that the cycloplatination occurred at the sp^3 carbon group for this complexation reaction due to the disappearance of the secondary proton peak from the ligand at 5.42 ppm. Since this carbon lost its proton from the C-H activation, this peak was not observed in the complex's spectra. Also, the peak belonging to the protons of the methyl groups was a doublet in the ligand, but after the cycloplatination, the splitting pattern went to a singlet due to the loss of the adjacent proton. The aromatic region is also noticeably different in the distribution of the aromatic protons. The crude reaction mixture was also examined using NMR to determine the ratio of sp^3 to sp^2 product formation. It was found that the ratio of sp^3 to sp^2 from this reaction was 100:0; it should also be stated that there was no formation of complex **3C**. The low yield from this reaction was due to the formation of two side products, one of which

resulted from a reaction with the solvent (**Scheme 9**), which will be discussed in chapter 5. As stated above, the poor yield of this reaction and the side reactions with the solvent prompted the use of a different solvent for complexation. The products from these reactions produced a switch in selectivity, which led to the formation of a different isomer.

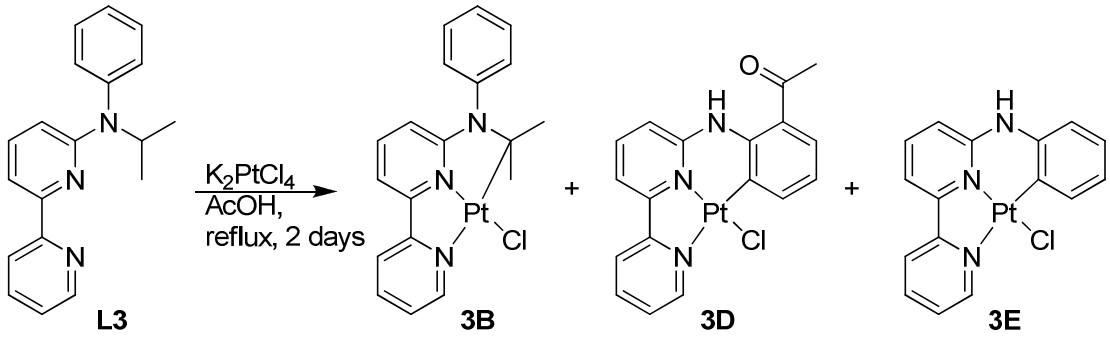

Scheme 9: Reaction of **L3** with K_2PtCl_4 in AcOH showing side products

Complexation of the Methyl Ligand (L1) in CH_3CN

The methyl ligand, **L1**, was complexed with potassium tetrachloroplatinate (K_2PtCl_4) in CH_3CN (**Scheme 10**). **Scheme 10** illustrates the two possible isomers from this reaction. After characterization, it was found that the major product was that of **1B** with a 73% yield after purification. The isomer was able to be characterized by comparing the NMR spectra of both **L1** and the purified product (**1B**) from this reaction (**Figure 23**).

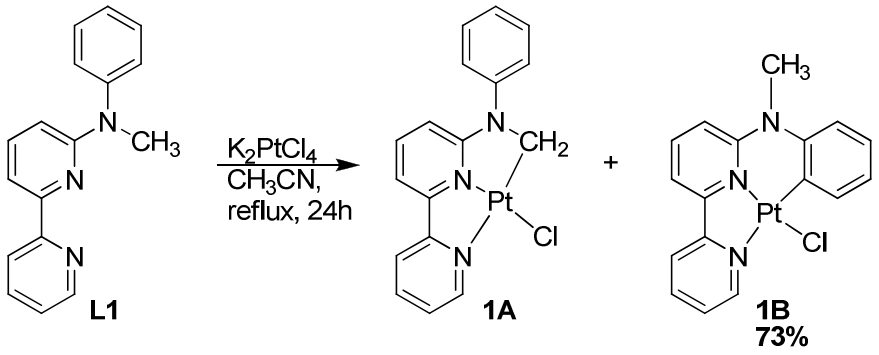

Scheme 10: Possible isomers of the complexation of **L1** in CH_3CN

The peak for the protons of the methyl group of the ligand shows up at 3.61 ppm and is a singlet. The peak for the same protons in the complex has been shifted downfield and now shows up at 3.74 ppm and again is a singlet. The aromatic region of these spectra gives a good indication that complexation has occurred as they are distinctly different when studying the distribution of the peaks from the aromatic protons, especially the proton that has been shifted far downfield to 9.78 ppm, as well as the peak at 6.59 ppm from the ligand that has been shifted downfield, by the platinum's sp^2 C-H bond activation. After integration of the spectra, the loss of one of the aromatic protons was the main indication that sp^2 C-H bond activation took place.

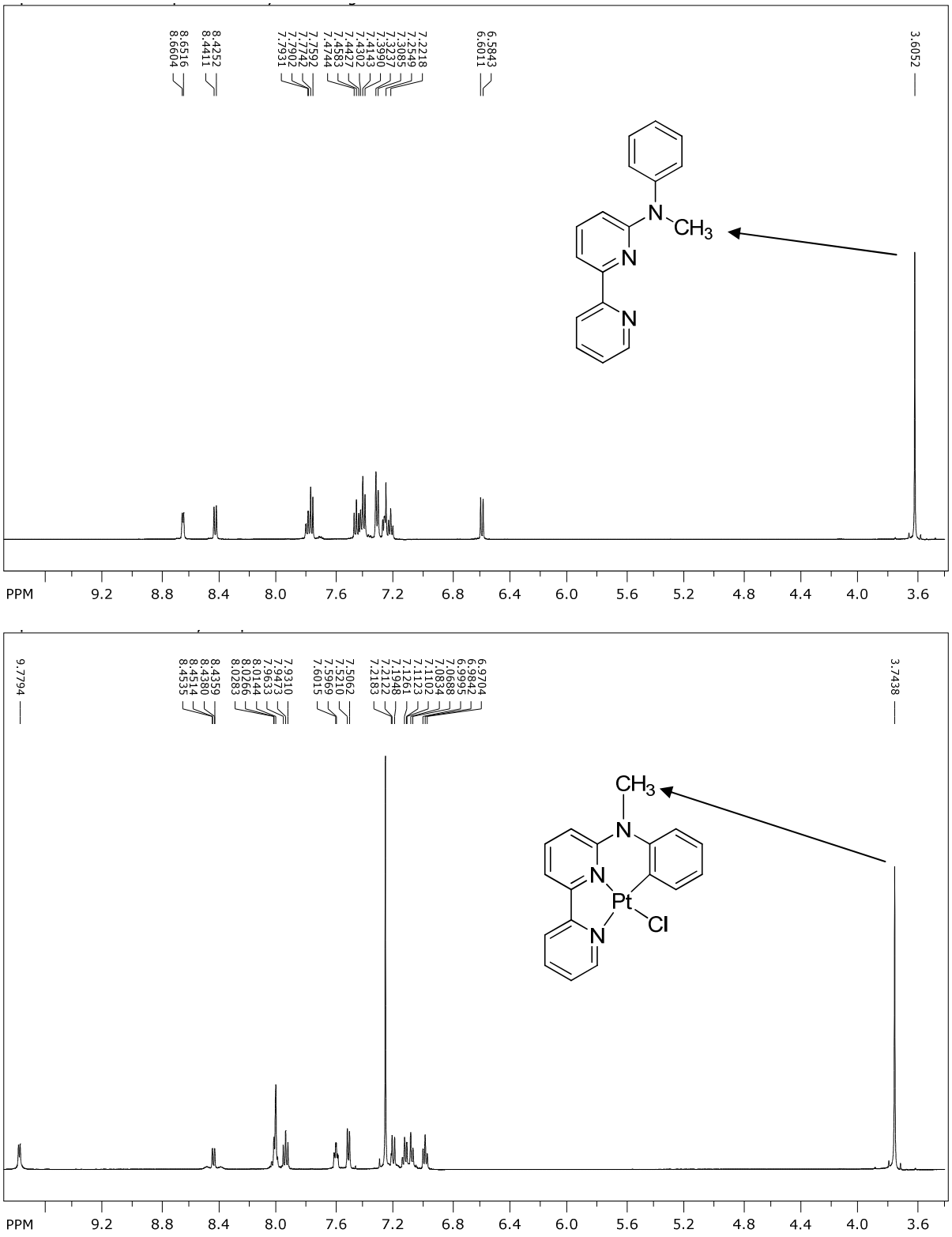

Figure 23: Comparison of **L1**'s (top) and complex **1B**'s (bottom) NMR spectrums

From these NMRs, it was possible to identify the product of the complexation reaction of **L1** in CH_3CN as being the sp^2 substituted product, where the C-H bond in the phenyl group was activated by the platinum metal. The crude reaction mixture was also examined using NMR to determine the ratio of sp^3 to sp^2 product formation. It was found that the ratio of sp^3 to sp^2 from this reaction was 0:100.

Complexation of the Ethyl Ligand (L2) in CH_3CN

The ethyl ligand, **L2**, was complexed with potassium tetrachloroplatinate (K_2PtCl_4) in CH_3CN (**Scheme 11**). **Scheme 11** illustrates the three possible isomers from this reaction. After characterization, it was found that the major product was that of **2B** with a 70% yield after purification. The isomer was able to be characterized by comparing the NMR spectra of both **L2** and the purified product (**2B**) from this reaction (**Figure 24**).

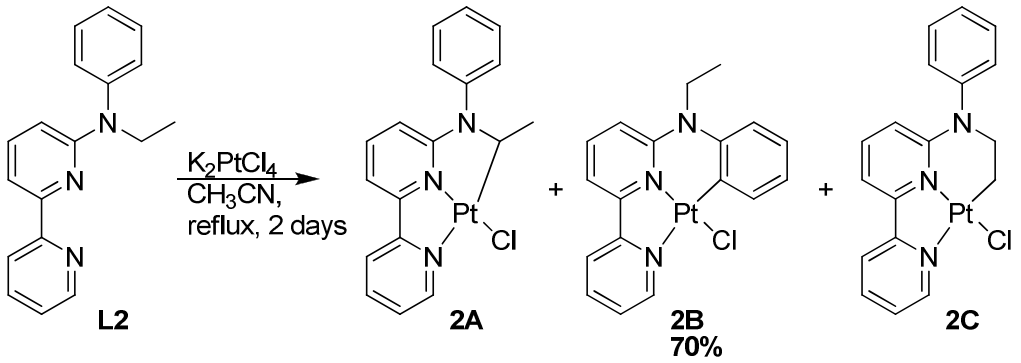

Scheme 11: Possible isomers of the complexation of **L2** in CH_3CN

The peak for the protons of the methyl group in the ligand is observed at 1.31 ppm and splits into a triplet, while the peak for the primary carbons's protons is seen at 4.15 ppm and splits to form a quartet. The peak for the protons of the methyl group of the complex have

shifted downfield to 1.44 ppm and has a triplet for its multiplicity. The peak for the protons of the primary carbon has also been shifted downfield to 4.26 ppm and splits into a quartet.

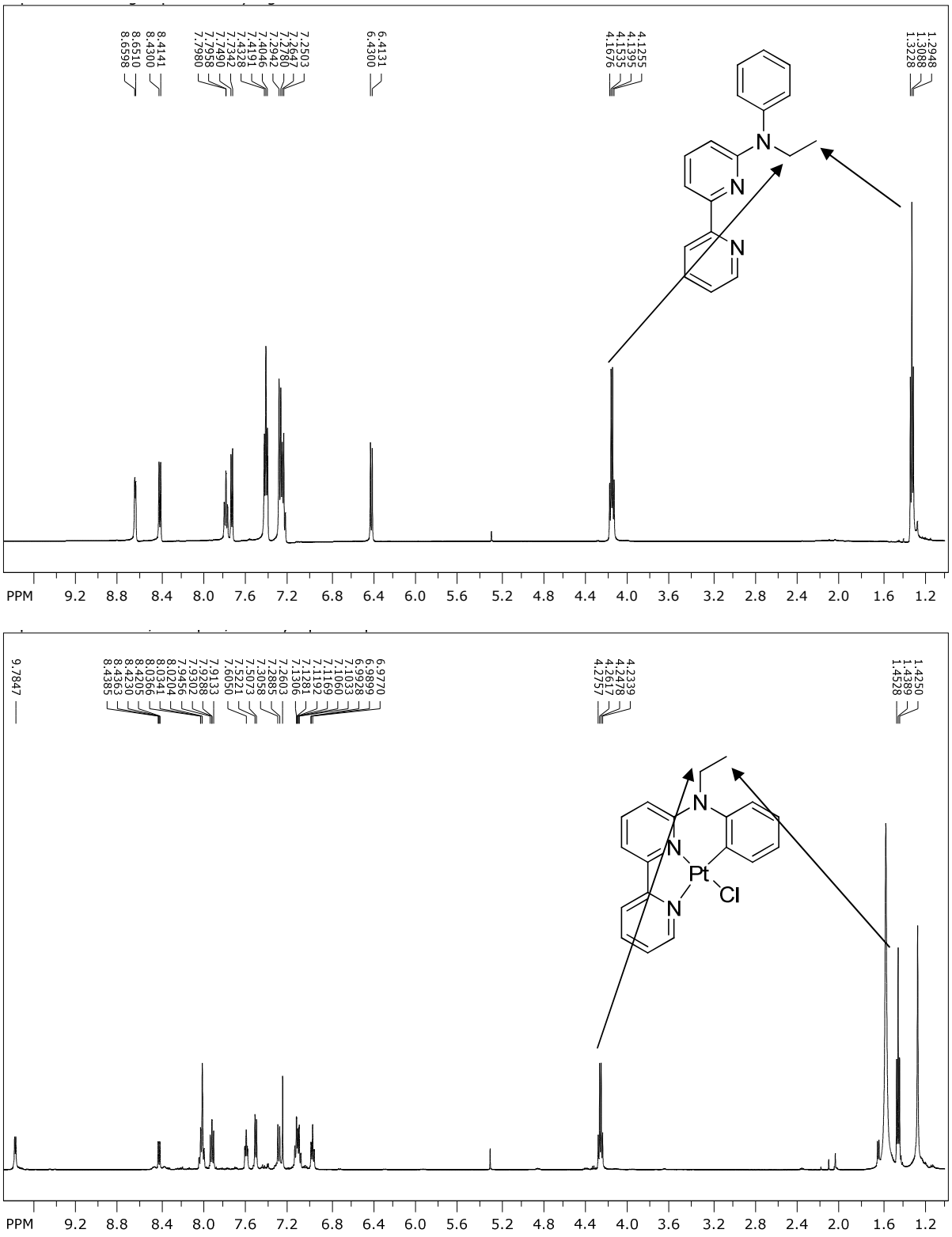

Figure 24: Comparison of **L2**'s (top) and complex **2B**'s (bottom) NMR spectra

After examining the NMR spectra, it is evident that the sp^2 C-H bond has been activated. This can be determined not only from the different distribution of the aromatic proton's peaks, but also the integration of the aromatic protons. It was found that one of the protons in the aromatic region had disappeared, indicating that the C-H bond on the phenyl group was activated. Another way to tell that the reaction did not occur on the alkyl group is that the splitting patterns of the complex and the ligand are still identical. The crude reaction mixture was also examined using NMR to determine the ratio of sp^3 to sp^2 product formation. It was found that the ratio of sp^3 to sp^2 from this reaction was 7:93, it should also be stated that there was no formation of complex **2C**.

Complexation of the Isopropyl Ligand (L3) in CH_3CN

The isopropyl ligand, **L3**, was complexed with potassium tetrachloroplatinate (K_2PtCl_4) in CH_3CN (**Scheme 12**). **Scheme 12** illustrates the three possible isomers from this reaction. After characterization, it was found that the major product was that of **3B** with a 36% yield after purification. The isomer was able to be characterized by comparing the NMR spectra of both **L3** and the purified product (**3B**) from this reaction (**Figure 25**).

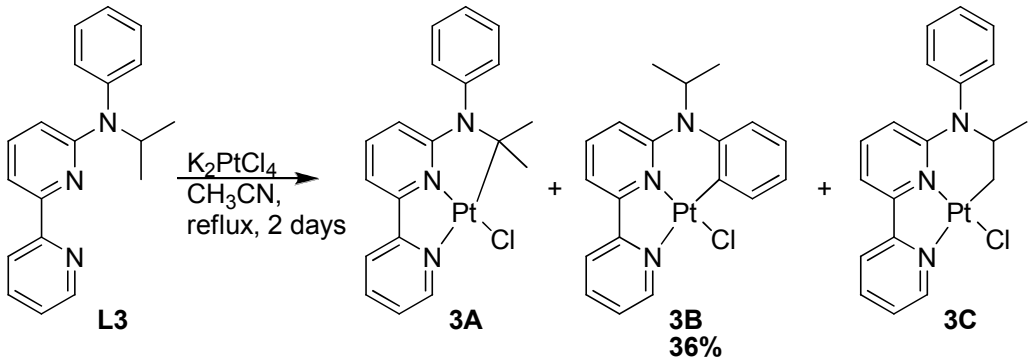

Scheme 12: Possible isomers of the complexation of **L3** in CH_3CN

The peak for the protons of the methyl groups in the ligand are evident at 1.22 ppm and splits into a doublet, while the peak for the secondary carbons's protons is seen at 5.42 ppm and splits to form a septet. The peak for the protons of the methyl groups of the complex have shifted downfield and shows up at 1.60 ppm and has a doublet for its multiplicity. The peak for the protons of the secondary carbons's proton has shifted upfield, showing up at 4.37 ppm and splits to form a septet.

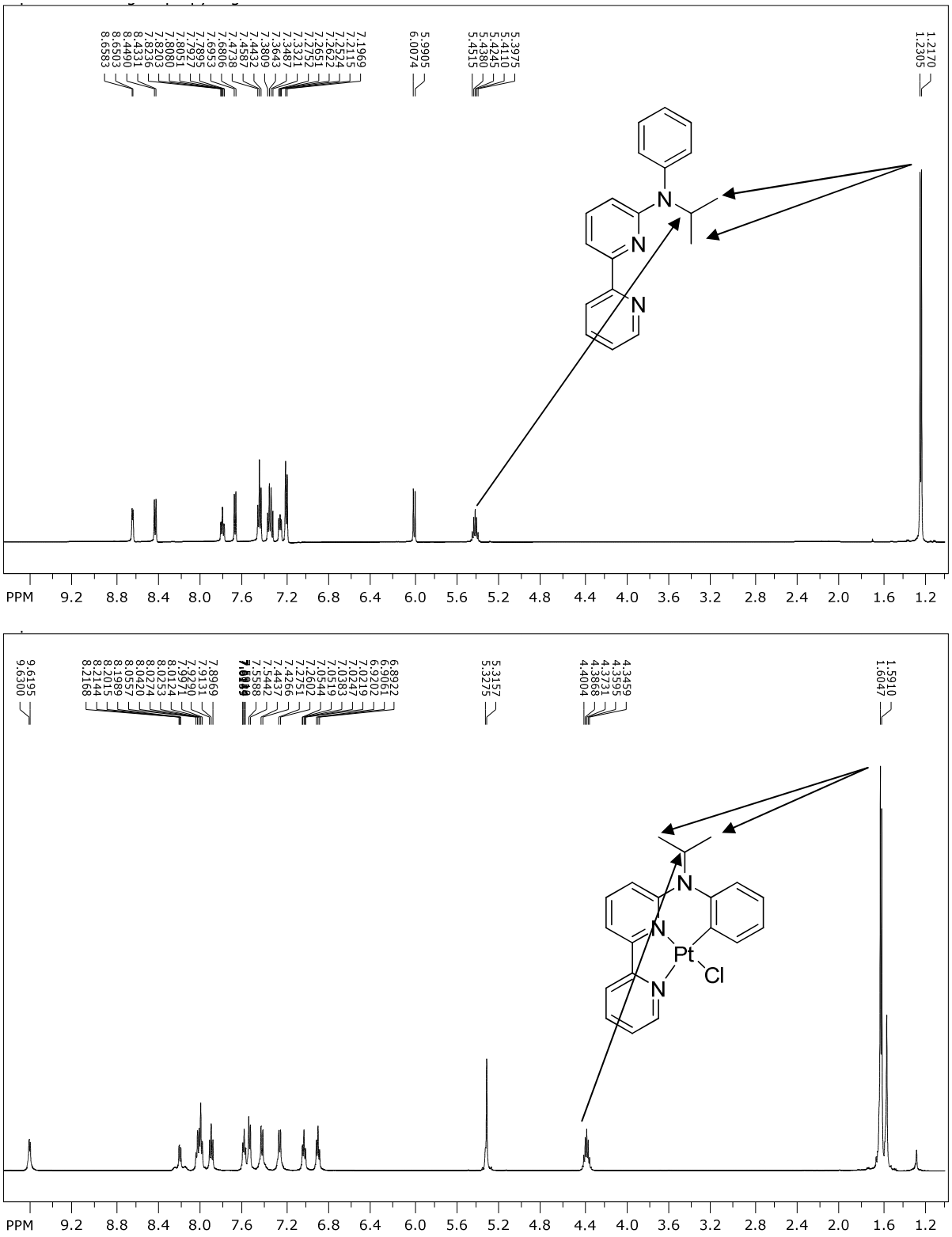

Figure 25: Comparison of **L3**'s (top) and complex **3A**'s (bottom) NMR spectra

After comparing these spectra, it is evident that the sp^2 C-H bond has been activated. Not only has the methyl group's proton peak been shifted downfield, but the secondary proton has been shifted up field. Both of the alkyl peaks also retained their splitting patterns that they had in the ligand's NMR spectrum. The comparison of the aromatic regions demonstrates the fact that the platinum has activated the sp^2 C-H bond on the phenyl group due to the different distribution of the aromatic proton's peaks. When the integration of the aromatic peaks were examined a loss of a proton was observed, which could only occur if the platinum were to activate the sp^2 C-H bond. The crude reaction mixture was also examined using NMR to determine the ratio of sp^3 to sp^2 product formation. It was found that the ratio of sp^3 to sp^2 from this reaction was 30:70, it should also be stated that there was no formation of complex **3C**.

Summary of Data Obtained

The following table, **Table 1**, summarizes all of the data collected though the synthesis and characterization process of this project. The most important data to take away from this table is the ratio of the isomers from each reaction, which was determined by proton NMR spectra of the crude product, and the yield, which is the isolated yield of the pure major isomer from the reaction.

Table 1: The reactions of **L1-L3** with K_2PtCl_4 in different solvents

Product	In AcOH			In MeCN		
	t (h)	Ratio[a]	Yield[b]	t (h)	Ratio[a]	Yield[b]
1A :**1B**	24	96:4	73%	72	0:100	73%
2A : **2B**	48	97:3	63%	48	7:93	70%
3A : **3B**	48	100:0	38%	72	30:70	36%

[a] Isomeric ratio determined by proton NMR spectra of the crude products; [b] Isolated yield of the pure major isomer.

X-Ray Crystallography

X-ray crystal structure determination was also performed on both of the isomers of the isopropyl complexes (**3A** and **3B**). X-ray crystallography has been one of the most notable techniques utilized in structure determination and it is rare to find studies of newly synthesized inorganic or organometallic complexes without a crystal structure for its characterization purposes. The difficulty in preparing a crystal for X-ray crystallography is the poor solubility of these complexes, which makes growing crystals of high quality rather difficult and tedious. The crystals reported here were grown by slow diffusion of hexane into a solution of dichloromethane or the evaporation technique of growing crystals with hexane and dichloromethane.

*Crystal Structure of Complex **3A***

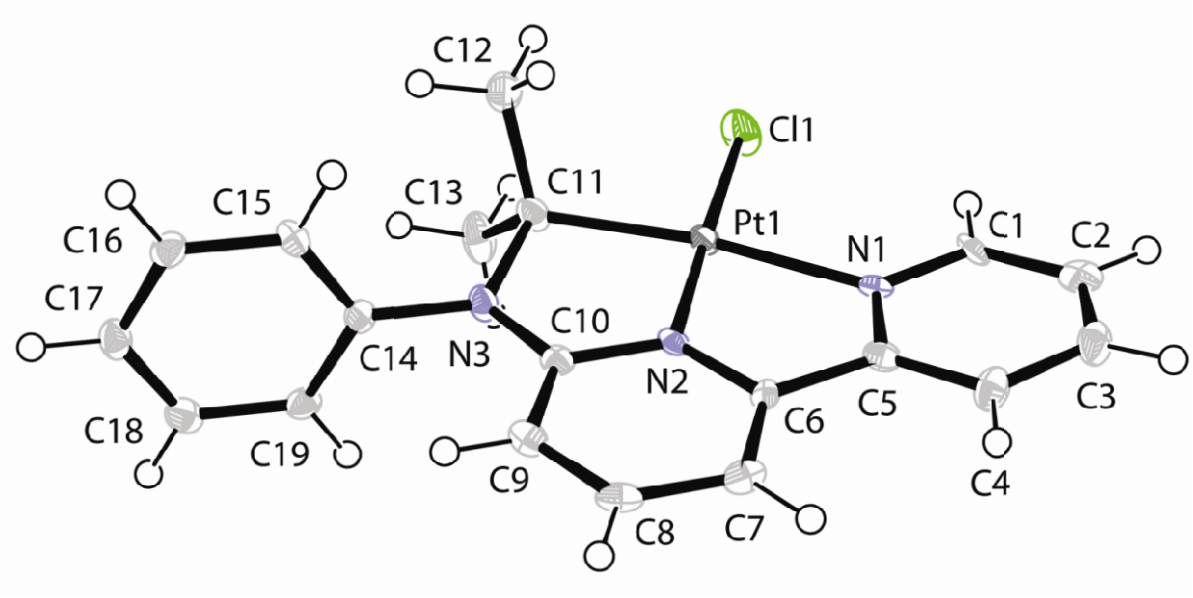

Figure 26: ORTEP diagram of complex **3A**, showing atomic numbering scheme

Table 2: Crystal data and structure refinement for complex **3A**

Identification code	pbca	
Empirical formula	C19 H18 Cl N3 Pt	
Formula weight	518.90	
Temperature	100(2) K	
Wavelength	1.54178 Å	
Crystal system	Orthorhombic	
Space group	Pbca	
Unit cell dimensions	a = 8.1377(2) Å	□= 90°.
	b = 16.8436(5) Å	□= 90°.
	c = 24.7285(6) Å	□ = 90°.
Volume	3389.49(15) $Å^3$	
Z	8	
Density (calculated)	2.034 Mg/m^3	
Absorption coefficient	16.965 mm^{-1}	
F(000)	1984	
Crystal size	0.34 x 0.19 x 0.16 mm^3	
Theta range for data collection	3.57 to 67.00°.	
Index ranges	-9<=h<=9, -19<=k<=17, -28<=l<=29	
Reflections collected	34181	
Independent reflections	3015 [R(int) = 0.0405]	
Completeness to theta = 67.00°	99.8 %	
Absorption correction	Numerical	
Max. and min. transmission	0.1746 and 0.0682	
Refinement method	Full-matrix least-squares on F^2	
Data / restraints / parameters	3015 / 0 / 219	
Goodness-of-fit on F^2	1.153	
Final R indices [I>2sigma(I)]	R1 = 0.0323, wR2 = 0.0943	
R indices (all data)	R1 = 0.0331, wR2 = 0.0949	
Largest diff. peak and hole	1.093 and -1.716 $e.Å^{-3}$	

Table 3: Atomic coordinates (x 10^4) and equivalent isotropic displacement parameters ($Å^2$x 10^3)for complex **3A**. U(eq) is defined as one third of the trace of the orthogonalized U^{ij} tensor

	x	y	z	U(eq)
Pt(1)	1546(1)	5572(1)	4063(1)	13(1)
Cl(1)	2773(2)	4670(1)	3491(1)	27(1)
N(1)	2258(6)	5093(3)	4818(2)	13(1)
N(2)	469(6)	6308(3)	4554(2)	12(1)
N(3)	-457(6)	6884(3)	3781(2)	15(1)
C(1)	3265(7)	4482(3)	4921(3)	16(1)
C(2)	3774(8)	4302(4)	5434(3)	20(1)
C(3)	3275(8)	4760(5)	5868(3)	24(2)
C(4)	2174(8)	5377(4)	5771(3)	20(1)
C(5)	1703(7)	5531(4)	5239(3)	17(1)
C(6)	609(7)	6206(3)	5095(2)	11(1)
C(7)	-205(7)	6708(4)	5446(2)	17(1)
C(8)	-1130(8)	7332(4)	5217(2)	17(1)
C(9)	-1228(7)	7431(4)	4669(3)	17(1)
C(10)	-431(7)	6895(3)	4324(2)	13(1)
C(11)	698(7)	6309(4)	3478(2)	17(1)
C(12)	2116(8)	6779(4)	3232(3)	23(1)
C(13)	-298(9)	5906(4)	3030(3)	25(2)
C(14)	-1380(7)	7473(4)	3494(2)	15(1)
C(15)	-652(7)	8177(3)	3333(2)	15(1)
C(16)	-1547(7)	8740(4)	3042(3)	17(1)
C(17)	-3165(8)	8593(4)	2911(2)	19(1)
C(18)	-3909(8)	7888(4)	3072(2)	19(1)
C(19)	-3019(8)	7336(4)	3361(2)	16(1)

Table 4: Bond lengths [Å] and angles [°] for complex **3A**

Pt(1)-N(2)	1.944(5)
Pt(1)-C(11)	2.026(6)
Pt(1)-N(1)	2.115(5)
Pt(1)-Cl(1)	2.3029(15)
N(1)-C(1)	1.339(8)
N(1)-C(5)	1.353(8)
N(2)-C(6)	1.352(7)
N(2)-C(10)	1.356(8)
N(3)-C(10)	1.344(8)
N(3)-C(14)	1.432(8)
N(3)-C(11)	1.543(7)
C(1)-C(2)	1.369(10)
C(1)-H(1)	0.9500
C(2)-C(3)	1.381(10)
C(2)-H(2)	0.9500
C(3)-C(4)	1.393(10)
C(3)-H(3)	0.9500
C(4)-C(5)	1.395(9)
C(4)-H(4)	0.9500
C(5)-C(6)	1.487(8)
C(6)-C(7)	1.383(8)
C(7)-C(8)	1.412(9)
C(7)-H(7)	0.9500
C(8)-C(9)	1.368(9)
C(8)-H(8)	0.9500
C(9)-C(10)	1.401(8)
C(9)-H(9)	0.9500
C(11)-C(12)	1.526(9)
C(11)-C(13)	1.532(8)
C(12)-H(12A)	0.9800
C(12)-H(12B)	0.9800
C(12)-H(12C)	0.9800

C(13)-H(13A)	0.9800
C(13)-H(13B)	0.9800
C(13)-H(13C)	0.9800
C(14)-C(15)	1.384(9)
C(14)-C(19)	1.393(9)
C(15)-C(16)	1.395(9)
C(15)-H(15)	0.9500
C(16)-C(17)	1.378(9)
C(16)-H(16)	0.9500
C(17)-C(18)	1.391(10)
C(17)-H(17)	0.9500
C(18)-C(19)	1.379(9)
C(18)-H(18)	0.9500
C(19)-H(19)	0.9500

N(2)-Pt(1)-C(11)	84.4(2)
N(2)-Pt(1)-N(1)	79.32(19)
C(11)-Pt(1)-N(1)	163.1(2)
N(2)-Pt(1)-Cl(1)	178.26(14)
C(11)-Pt(1)-Cl(1)	96.53(17)
N(1)-Pt(1)-Cl(1)	99.88(13)
C(1)-N(1)-C(5)	118.4(5)
C(1)-N(1)-Pt(1)	128.9(4)
C(5)-N(1)-Pt(1)	112.3(4)
C(6)-N(2)-C(10)	123.6(5)
C(6)-N(2)-Pt(1)	119.9(4)
C(10)-N(2)-Pt(1)	116.5(4)
C(10)-N(3)-C(14)	119.6(5)
C(10)-N(3)-C(11)	118.9(5)
C(14)-N(3)-C(11)	121.0(5)
N(1)-C(1)-C(2)	122.2(6)
N(1)-C(1)-H(1)	118.9
C(2)-C(1)-H(1)	118.9
C(1)-C(2)-C(3)	120.4(6)

C(1)-C(2)-H(2)	119.8
C(3)-C(2)-H(2)	119.8
C(2)-C(3)-C(4)	118.2(6)
C(2)-C(3)-H(3)	120.9
C(4)-C(3)-H(3)	120.9
C(5)-C(4)-C(3)	118.5(6)
C(5)-C(4)-H(4)	120.8
C(3)-C(4)-H(4)	120.8
N(1)-C(5)-C(4)	122.2(6)
N(1)-C(5)-C(6)	115.6(6)
C(4)-C(5)-C(6)	122.2(6)
N(2)-C(6)-C(7)	120.2(5)
N(2)-C(6)-C(5)	112.6(5)
C(7)-C(6)-C(5)	127.2(5)
C(6)-C(7)-C(8)	117.3(5)
C(6)-C(7)-H(7)	121.3
C(8)-C(7)-H(7)	121.3
C(9)-C(8)-C(7)	121.3(6)
C(9)-C(8)-H(8)	119.4
C(7)-C(8)-H(8)	119.4
C(8)-C(9)-C(10)	119.8(6)
C(8)-C(9)-H(9)	120.1
C(10)-C(9)-H(9)	120.1
N(3)-C(10)-N(2)	114.7(5)
N(3)-C(10)-C(9)	127.5(5)
N(2)-C(10)-C(9)	117.7(5)
C(12)-C(11)-C(13)	110.0(5)
C(12)-C(11)-N(3)	109.1(5)
C(13)-C(11)-N(3)	107.8(5)
C(12)-C(11)-Pt(1)	110.2(4)
C(13)-C(11)-Pt(1)	115.2(4)
N(3)-C(11)-Pt(1)	104.3(4)
C(11)-C(12)-H(12A)	109.5
C(11)-C(12)-H(12B)	109.5

H(12A)-C(12)-H(12B)	109.5
C(11)-C(12)-H(12C)	109.5
H(12A)-C(12)-H(12C)	109.5
H(12B)-C(12)-H(12C)	109.5
C(11)-C(13)-H(13A)	109.5
C(11)-C(13)-H(13B)	109.5
H(13A)-C(13)-H(13B)	109.5
C(11)-C(13)-H(13C)	109.5
H(13A)-C(13)-H(13C)	109.5
H(13B)-C(13)-H(13C)	109.5
C(15)-C(14)-C(19)	119.0(6)
C(15)-C(14)-N(3)	120.8(5)
C(19)-C(14)-N(3)	120.2(6)
C(14)-C(15)-C(16)	120.4(6)
C(14)-C(15)-H(15)	119.8
C(16)-C(15)-H(15)	119.8
C(17)-C(16)-C(15)	119.9(6)
C(17)-C(16)-H(16)	120.1
C(15)-C(16)-H(16)	120.1
C(16)-C(17)-C(18)	120.1(6)
C(16)-C(17)-H(17)	119.9
C(18)-C(17)-H(17)	119.9
C(19)-C(18)-C(17)	119.7(6)
C(19)-C(18)-H(18)	120.2
C(17)-C(18)-H(18)	120.2
C(18)-C(19)-C(14)	120.9(6)
C(18)-C(19)-H(19)	119.6
C(14)-C(19)-H(19)	119.6

*Crystal Structure of Complex **3B***

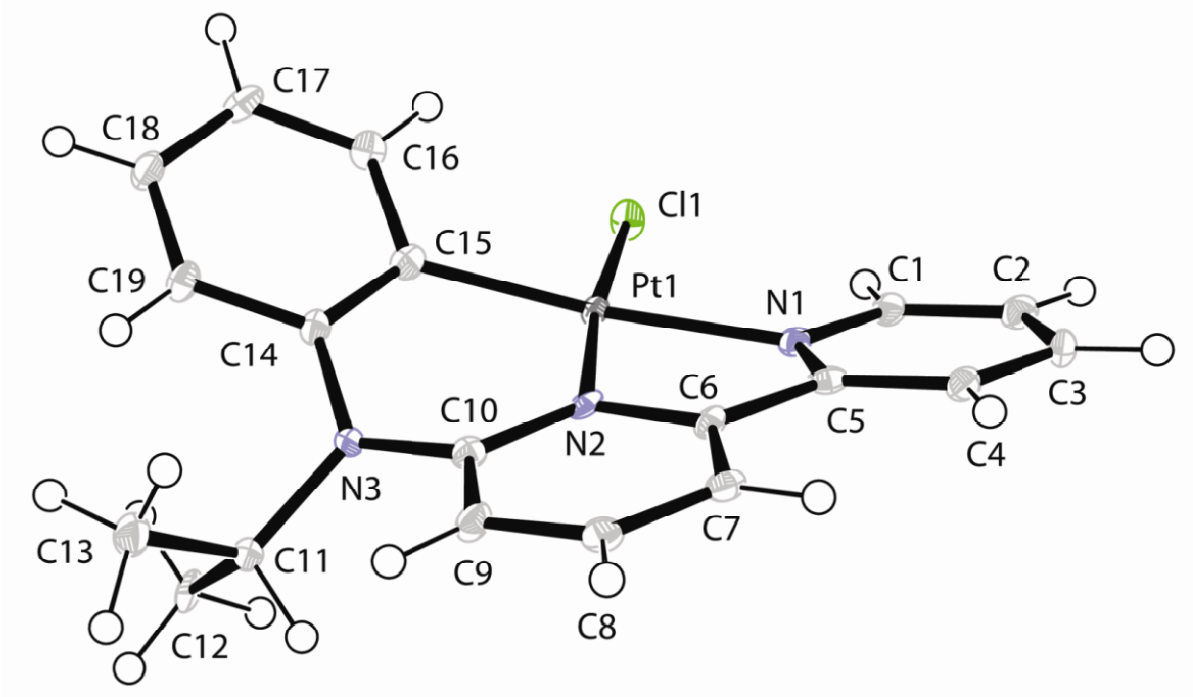

Figure 27: ORTEP diagram of complex **3B**, showing atomic numbering scheme.

Table 5: Crystal data and structure refinement for complex **3B**

Identification code	p1bar	
Empirical formula	C19 H18 Cl N3 Pt	
Formula weight	518.90	
Temperature	100(2) K	
Wavelength	1.54178 Å	
Crystal system	Triclinic	
Space group	P-1	
Unit cell dimensions	a = 7.6378(2) Å	□= 88.2820(10)°.
	b = 14.7260(3) Å	□= 84.6860(10)°.
	c = 15.0539(3) Å	□ = 81.3120(10)°.
Volume	1666.33(6) $Å^3$	
Z	4	
Density (calculated)	2.068 Mg/m^3	
Absorption coefficient	17.254 mm^{-1}	
F(000)	992	
Crystal size	0.35 x 0.28 x 0.14 mm^3	
Theta range for data collection	2.95 to 67.00°.	
Index ranges	-8<=h<=9, -17<=k<=17, -17<=l<=17	
Reflections collected	28251	
Independent reflections	5766 [R(int) = 0.0378]	
Completeness to theta = 67.00°	97.1 %	
Absorption correction	Numerical	
Max. and min. transmission	0.1993 and 0.0656	
Refinement method	Full-matrix least-squares on F^2	
Data / restraints / parameters	5766 / 0 / 436	
Goodness-of-fit on F^2	1.144	
Final R indices [I>2sigma(I)]	R1 = 0.0325, wR2 = 0.0844	
R indices (all data)	R1 = 0.0329, wR2 = 0.0846	
Largest diff. peak and hole	0.895 and -3.507 $e.Å^{-3}$	

Table 6: Atomic coordinates (x 10^4) and equivalent isotropic displacement parameters ($Å^2$x 10^3) for complex **3B**. U(eq) is defined as one third of the trace of the orthogonalized U^{ij} tensor

	x	y	z	U(eq)
Pt(1)	4449(1)	6617(1)	6083(1)	9(1)
Pt(2)	1192(1)	8664(1)	1049(1)	10(1)
Cl(1)	5359(2)	8045(1)	5946(1)	14(1)
Cl(2)	998(2)	7114(1)	941(1)	16(1)
N(1)	3160(5)	6795(3)	4910(3)	11(1)
N(2)	3462(5)	5433(3)	6103(3)	10(1)
N(3)	4028(5)	5030(3)	7599(3)	11(1)
N(4)	2646(6)	8699(3)	-190(3)	14(1)
N(5)	1549(6)	9981(3)	1016(3)	13(1)
N(6)	572(6)	10284(3)	2540(3)	12(1)
C(1)	3060(6)	7517(3)	4347(3)	13(1)
C(2)	2467(7)	7489(4)	3512(4)	15(1)
C(3)	1990(7)	6680(4)	3226(3)	16(1)
C(4)	2103(6)	5925(4)	3814(3)	13(1)
C(5)	2678(6)	6003(3)	4652(3)	12(1)
C(6)	2768(6)	5258(3)	5328(3)	11(1)
C(7)	2119(6)	4449(3)	5215(3)	13(1)
C(8)	2145(7)	3809(3)	5912(3)	13(1)
C(9)	2740(7)	4012(4)	6707(4)	14(1)
C(10)	3435(6)	4833(3)	6802(3)	11(1)
C(11)	3113(7)	4641(4)	8419(3)	15(1)
C(12)	2766(7)	5353(4)	9165(3)	20(1)
C(13)	3970(7)	3696(4)	8761(4)	20(1)
C(14)	5563(7)	5468(3)	7654(3)	11(1)
C(15)	5937(7)	6187(3)	7080(3)	13(1)
C(16)	7566(7)	6506(3)	7132(3)	14(1)
C(17)	8754(7)	6155(4)	7744(4)	16(1)
C(18)	8307(7)	5466(4)	8341(3)	16(1)
C(19)	6739(7)	5129(4)	8291(3)	14(1)

C(20)	3104(7)	7998(4)	-765(4)	19(1)
C(21)	3853(8)	8131(4)	-1623(4)	24(1)
C(22)	4132(7)	9007(4)	-1898(4)	21(1)
C(23)	3678(7)	9726(4)	-1310(4)	16(1)
C(24)	2908(6)	9552(4)	-455(4)	15(1)
C(25)	2336(7)	10271(4)	213(3)	14(1)
C(26)	2612(7)	11164(4)	71(4)	17(1)
C(27)	2089(7)	11796(4)	747(4)	16(1)
C(28)	1385(7)	11497(4)	1552(4)	15(1)
C(29)	1144(7)	10572(4)	1707(4)	14(1)
C(30)	1195(7)	10748(3)	3300(3)	12(1)
C(31)	-122(8)	11523(4)	3745(4)	22(1)
C(32)	1954(7)	10036(4)	3968(3)	17(1)
C(33)	-567(6)	9599(3)	2712(3)	12(1)
C(34)	-1845(7)	9732(4)	3435(4)	15(1)
C(35)	-3049(7)	9121(4)	3639(4)	17(1)
C(36)	-3004(7)	8378(4)	3085(4)	17(1)
C(37)	-1745(7)	8249(4)	2370(4)	15(1)
C(38)	-465(6)	8838(3)	2162(3)	11(1)

Table 7: Bond lengths [Å] and angles [°] for complex **3B**

Pt(1)-N(2)	2.000(4)
Pt(1)-C(15)	1.997(5)
Pt(1)-N(1)	2.091(4)
Pt(1)-Cl(1)	2.3100(11)
Pt(2)-N(5)	1.997(4)
Pt(2)-C(38)	2.002(5)
Pt(2)-N(4)	2.085(4)
Pt(2)-Cl(2)	2.3214(12)
N(1)-C(1)	1.338(7)
N(1)-C(5)	1.352(7)
N(2)-C(10)	1.354(7)
N(2)-C(6)	1.371(7)
N(3)-C(10)	1.375(7)
N(3)-C(14)	1.431(6)
N(3)-C(11)	1.503(6)
N(4)-C(24)	1.345(7)
N(4)-C(20)	1.351(7)
N(5)-C(29)	1.360(7)
N(5)-C(25)	1.384(7)
N(6)-C(29)	1.365(7)
N(6)-C(33)	1.432(6)
N(6)-C(30)	1.500(6)
C(1)-C(2)	1.379(8)
C(1)-H(1)	0.9500
C(2)-C(3)	1.388(8)
C(2)-H(2)	0.9500
C(3)-C(4)	1.398(7)
C(3)-H(3)	0.9500
C(4)-C(5)	1.388(7)
C(4)-H(4)	0.9500
C(5)-C(6)	1.471(7)
C(6)-C(7)	1.379(7)

C(7)-C(8)	1.389(7)
C(7)-H(7)	0.9500
C(8)-C(9)	1.376(8)
C(8)-H(8)	0.9500
C(9)-C(10)	1.408(7)
C(9)-H(9)	0.9500
C(11)-C(12)	1.538(8)
C(11)-C(13)	1.541(7)
C(11)-H(11)	1.0000
C(12)-H(12A)	0.9800
C(12)-H(12B)	0.9800
C(12)-H(12C)	0.9800
C(13)-H(13A)	0.9800
C(13)-H(13B)	0.9800
C(13)-H(13C)	0.9800
C(14)-C(15)	1.393(7)
C(14)-C(19)	1.404(7)
C(15)-C(16)	1.404(7)
C(16)-C(17)	1.386(7)
C(16)-H(16)	0.9500
C(17)-C(18)	1.396(8)
C(17)-H(17)	0.9500
C(18)-C(19)	1.373(8)
C(18)-H(18)	0.9500
C(19)-H(19)	0.9500
C(20)-C(21)	1.384(8)
C(20)-H(20)	0.9500
C(21)-C(22)	1.385(9)
C(21)-H(21)	0.9500
C(22)-C(23)	1.383(8)
C(22)-H(22)	0.9500
C(23)-C(24)	1.397(8)
C(23)-H(23)	0.9500
C(24)-C(25)	1.473(8)

C(25)-C(26)	1.370(8)
C(26)-C(27)	1.390(8)
C(26)-H(26)	0.9500
C(27)-C(28)	1.367(8)
C(27)-H(27)	0.9500
C(28)-C(29)	1.411(7)
C(28)-H(28)	0.9500
C(30)-C(32)	1.519(7)
C(30)-C(31)	1.529(7)
C(30)-H(30)	1.0000
C(31)-H(31A)	0.9800
C(31)-H(31B)	0.9800
C(31)-H(31C)	0.9800
C(32)-H(32A)	0.9800
C(32)-H(32B)	0.9800
C(32)-H(32C)	0.9800
C(33)-C(34)	1.390(8)
C(33)-C(38)	1.402(7)
C(34)-C(35)	1.390(8)
C(34)-H(34)	0.9500
C(35)-C(36)	1.389(8)
C(35)-H(35)	0.9500
C(36)-C(37)	1.374(8)
C(36)-H(36)	0.9500
C(37)-C(38)	1.410(7)
C(37)-H(37)	0.9500

N(2)-Pt(1)-C(15)	91.67(19)
N(2)-Pt(1)-N(1)	80.70(17)
C(15)-Pt(1)-N(1)	167.32(18)
N(2)-Pt(1)-Cl(1)	173.54(12)
C(15)-Pt(1)-Cl(1)	94.73(15)
N(1)-Pt(1)-Cl(1)	93.13(12)
N(5)-Pt(2)-C(38)	92.12(19)

N(5)-Pt(2)-N(4)	80.83(18)
C(38)-Pt(2)-N(4)	169.67(18)
N(5)-Pt(2)-Cl(2)	173.43(13)
C(38)-Pt(2)-Cl(2)	94.45(14)
N(4)-Pt(2)-Cl(2)	92.66(13)
C(1)-N(1)-C(5)	119.2(4)
C(1)-N(1)-Pt(1)	127.8(3)
C(5)-N(1)-Pt(1)	111.9(3)
C(10)-N(2)-C(6)	120.6(4)
C(10)-N(2)-Pt(1)	125.3(3)
C(6)-N(2)-Pt(1)	114.2(3)
C(10)-N(3)-C(14)	123.0(4)
C(10)-N(3)-C(11)	115.6(4)
C(14)-N(3)-C(11)	120.9(4)
C(24)-N(4)-C(20)	119.5(5)
C(24)-N(4)-Pt(2)	113.1(3)
C(20)-N(4)-Pt(2)	126.8(4)
C(29)-N(5)-C(25)	119.9(5)
C(29)-N(5)-Pt(2)	125.7(4)
C(25)-N(5)-Pt(2)	114.5(4)
C(29)-N(6)-C(33)	124.3(4)
C(29)-N(6)-C(30)	115.5(4)
C(33)-N(6)-C(30)	120.1(4)
N(1)-C(1)-C(2)	122.4(5)
N(1)-C(1)-H(1)	118.8
C(2)-C(1)-H(1)	118.8
C(1)-C(2)-C(3)	119.6(5)
C(1)-C(2)-H(2)	120.2
C(3)-C(2)-H(2)	120.2
C(2)-C(3)-C(4)	117.9(5)
C(2)-C(3)-H(3)	121.0
C(4)-C(3)-H(3)	121.0
C(5)-C(4)-C(3)	119.7(5)
C(5)-C(4)-H(4)	120.1

C(3)-C(4)-H(4)	120.1
N(1)-C(5)-C(4)	121.2(5)
N(1)-C(5)-C(6)	115.2(4)
C(4)-C(5)-C(6)	123.5(5)
C(7)-C(6)-N(2)	121.5(5)
C(7)-C(6)-C(5)	122.5(5)
N(2)-C(6)-C(5)	115.9(4)
C(6)-C(7)-C(8)	118.7(5)
C(6)-C(7)-H(7)	120.6
C(8)-C(7)-H(7)	120.6
C(7)-C(8)-C(9)	119.5(5)
C(7)-C(8)-H(8)	120.3
C(9)-C(8)-H(8)	120.3
C(8)-C(9)-C(10)	120.7(5)
C(8)-C(9)-H(9)	119.6
C(10)-C(9)-H(9)	119.6
N(2)-C(10)-N(3)	120.9(4)
N(2)-C(10)-C(9)	118.8(5)
N(3)-C(10)-C(9)	120.3(4)
N(3)-C(11)-C(12)	110.3(4)
N(3)-C(11)-C(13)	116.9(4)
C(12)-C(11)-C(13)	111.6(4)
N(3)-C(11)-H(11)	105.8
C(12)-C(11)-H(11)	105.8
C(13)-C(11)-H(11)	105.8
C(11)-C(12)-H(12A)	109.5
C(11)-C(12)-H(12B)	109.5
H(12A)-C(12)-H(12B)	109.5
C(11)-C(12)-H(12C)	109.5
H(12A)-C(12)-H(12C)	109.5
H(12B)-C(12)-H(12C)	109.5
C(11)-C(13)-H(13A)	109.5
C(11)-C(13)-H(13B)	109.5
H(13A)-C(13)-H(13B)	109.5

C(11)-C(13)-H(13C)	109.5
H(13A)-C(13)-H(13C)	109.5
H(13B)-C(13)-H(13C)	109.5
C(15)-C(14)-C(19)	120.1(5)
C(15)-C(14)-N(3)	122.0(4)
C(19)-C(14)-N(3)	117.8(4)
C(16)-C(15)-C(14)	117.3(5)
C(16)-C(15)-Pt(1)	119.9(4)
C(14)-C(15)-Pt(1)	122.0(4)
C(15)-C(16)-C(17)	122.7(5)
C(15)-C(16)-H(16)	118.7
C(17)-C(16)-H(16)	118.7
C(18)-C(17)-C(16)	118.9(5)
C(18)-C(17)-H(17)	120.6
C(16)-C(17)-H(17)	120.6
C(19)-C(18)-C(17)	119.6(5)
C(19)-C(18)-H(18)	120.2
C(17)-C(18)-H(18)	120.2
C(18)-C(19)-C(14)	121.4(5)
C(18)-C(19)-H(19)	119.3
C(14)-C(19)-H(19)	119.3
N(4)-C(20)-C(21)	121.7(5)
N(4)-C(20)-H(20)	119.1
C(21)-C(20)-H(20)	119.1
C(20)-C(21)-C(22)	118.9(5)
C(20)-C(21)-H(21)	120.5
C(22)-C(21)-H(21)	120.5
C(23)-C(22)-C(21)	119.5(5)
C(23)-C(22)-H(22)	120.2
C(21)-C(22)-H(22)	120.2
C(22)-C(23)-C(24)	118.9(5)
C(22)-C(23)-H(23)	120.5
C(24)-C(23)-H(23)	120.5
N(4)-C(24)-C(23)	121.3(5)

N(4)-C(24)-C(25)	115.4(5)
C(23)-C(24)-C(25)	123.2(5)
C(26)-C(25)-N(5)	121.6(5)
C(26)-C(25)-C(24)	122.8(5)
N(5)-C(25)-C(24)	115.5(5)
C(25)-C(26)-C(27)	119.4(5)
C(25)-C(26)-H(26)	120.3
C(27)-C(26)-H(26)	120.3
C(28)-C(27)-C(26)	118.7(5)
C(28)-C(27)-H(27)	120.6
C(26)-C(27)-H(27)	120.6
C(27)-C(28)-C(29)	121.9(5)
C(27)-C(28)-H(28)	119.0
C(29)-C(28)-H(28)	119.0
N(6)-C(29)-N(5)	121.6(5)
N(6)-C(29)-C(28)	120.1(5)
N(5)-C(29)-C(28)	118.2(5)
N(6)-C(30)-C(32)	110.2(4)
N(6)-C(30)-C(31)	116.5(4)
C(32)-C(30)-C(31)	112.5(4)
N(6)-C(30)-H(30)	105.5
C(32)-C(30)-H(30)	105.5
C(31)-C(30)-H(30)	105.5
C(30)-C(31)-H(31A)	109.5
C(30)-C(31)-H(31B)	109.5
H(31A)-C(31)-H(31B)	109.5
C(30)-C(31)-H(31C)	109.5
H(31A)-C(31)-H(31C)	109.5
H(31B)-C(31)-H(31C)	109.5
C(30)-C(32)-H(32A)	109.5
C(30)-C(32)-H(32B)	109.5
H(32A)-C(32)-H(32B)	109.5
C(30)-C(32)-H(32C)	109.5
H(32A)-C(32)-H(32C)	109.5

H(32B)-C(32)-H(32C)	109.5
C(34)-C(33)-C(38)	120.4(5)
C(34)-C(33)-N(6)	117.3(5)
C(38)-C(33)-N(6)	122.2(5)
C(33)-C(34)-C(35)	121.6(5)
C(33)-C(34)-H(34)	119.2
C(35)-C(34)-H(34)	119.2
C(36)-C(35)-C(34)	118.7(5)
C(36)-C(35)-H(35)	120.6
C(34)-C(35)-H(35)	120.6
C(37)-C(36)-C(35)	119.5(5)
C(37)-C(36)-H(36)	120.2
C(35)-C(36)-H(36)	120.2
C(36)-C(37)-C(38)	123.2(5)
C(36)-C(37)-H(37)	118.4
C(38)-C(37)-H(37)	118.4
C(33)-C(38)-C(37)	116.5(5)
C(33)-C(38)-Pt(2)	122.5(4)
C(37)-C(38)-Pt(2)	120.6(4)

The complex **3A** displays a planar coordination geometry. The N-phenyl group is nearly perpendicular to the coordination plane, which is to minimize the steric interaction with the isopropyl and bipyridyl groups. The complex **3B** has a N^N*C coordination geometry featuring a fused five-six-membered metallacycle, where N*C denotes a six-membered and N^N denotes a five-membered chelation to the platinum. In contrast to **3A**, the tridentate chelating ligand in **3B** is not planar and the N-phenyl group is significantly bent with respect to the rest of the coordination geometry. This geometric distortion from desired square planar structure of Pt(II) complexes is likely the result of the steric hindrance

caused by the isopropyl group, since in a similar five-six-membered platinacycle where all three N-substituents are either phenyl or pyridine rings, the coordination geometry is closer to a square plane.[20]

CHAPTER 4: MECHANISTIC STUDIES

After the characterization of the complexes, the focus of the research turned to revealing the underlying factors responsible for the interesting selectivity in intramolecular C-H bond activation. It was reasoned that the reactions in AcOH might be thermodynamically controlled while the reaction in acetonitrile might be kinetically controlled. Therefore, several mechanistic studies were performed on the complexes in order to determine the validity of this reasoning. The general notion of preference of sp^2 C-H bond activation has been accepted; however, the complex formed through sp^3 C-H bond activation may be more stable than that through the sp^2 C-H activation because of the formation of a five-membered chelate. Five-membered metal chelation is generally more stable than the chelation of other sizes in coordination complexes.[46] Another major contributing factor is steric interaction of the pendent N-alkyl group with the tridentate chelating ligand. For complexes **1A-3A**, the pendent N-phenyl group is able to adopt a perpendicular orientation relative to the rest of the complex in order to minimize the steric interaction.

The studies performed for this portion of the research include isomerization reactions of complexes **1A** and **1B**, as well as a reaction and isomerizations in deuterated acetic acid (AcOD).

Isomerization Reactions

*Isomerization of **1B** to **1A***

To confirm the hypothesis of thermodynamic control of the reaction in acetic acid, pure complex **1B** was refluxed in acetic acid (**Scheme 13**). The Isomerization to **1A** proceeded slowly but to near completion after three days (**1A:1B** = 96:4 from the NMR of the crude reaction mixture).

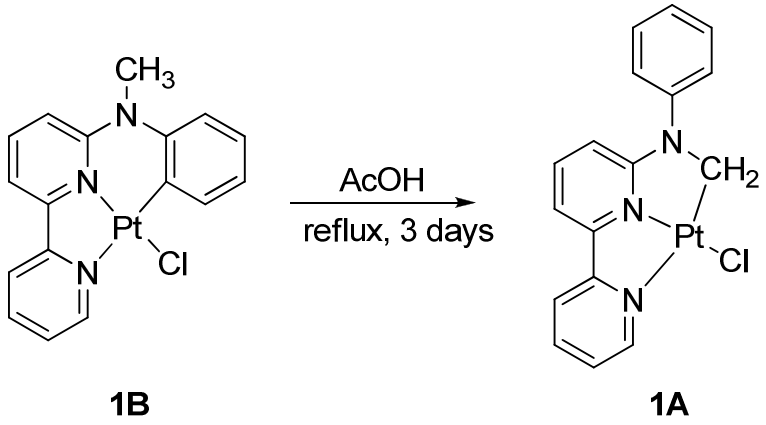

1B **1A**

Scheme 13: Isomerization of **1B** to **1A** in AcOH

The Isomerization of this complex is likely taking place via an acid-assisted cleavage of the Pt-C (sp^2) bond from **1B**, followed by the C-H bond activation of the methyl group (sp^3) by the platinum center, to give the other isomer, **1A**.

*Isomerization of **1A** to **1B***

It was fairly certain that an isomerization of **1A** to **1B** would not occur; however, the reaction was carried out to support our claim that the sp^3 substituted complex was the thermodynamic controlled product. Similar to the previous isomerization, complex **1A** was refluxed in acetonitrile for three days (**Scheme 14**), and when the crude reaction mixture was examined using NMR, it was determined that no isomerization to **1B** took place.

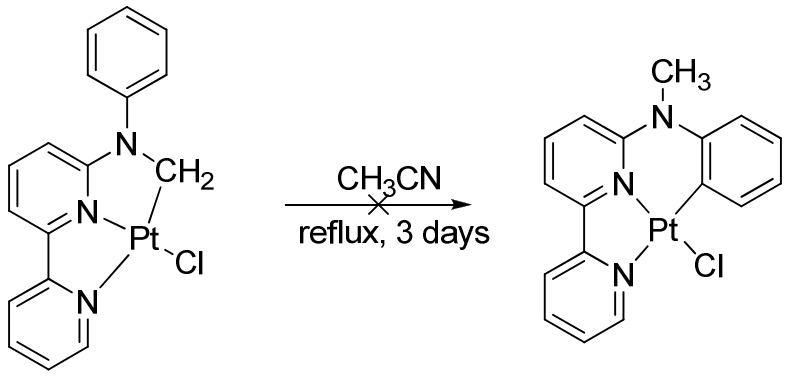

1A **1B**

Scheme 14: Isomerization of **1A** to **1B** in acetonitrile

To try to force the isomerization to occur, a 1:1 molar ratio of HCl to complex **1A** was again refluxed in acetonitrile in an attempt to allow the acid-assisted cleavage of the Pt-C (sp^3) bond from **1A**. HCl was chosen due to the fact that HCl is a strong acid that could hydrolyze the C-Pt bond to allow the isomerization to take place. However, after examining the NMR spectra of the crude reaction mixture, no isomerization was evident.

Reaction, Isomerization and H/D Exchange in AcOD

When the reaction of **L1** with K_2PtCl_4 was carried out in AcOD, a high degree of deuterium incorporation was found at the *ortho* positions of the N-phenyl ring and the methylene group, along with partial H/D exchange detected on the pyridine ring as shown in **Scheme 15**. The H/D exchange at the *ortho*-position of the N-phenyl ring and the methylene group may be interpreted by reversible bipyridine-directed cycloplatination reaction. The H/D exchange on the pyridine ring is likely attained through the bidentate cyclometalation of the bipyridine ligand.[47] When the isomerisation of **1B** was carried out in AcOD, a similar level of H/D exchange at the *ortho* position of the N-phenyl ring and the methylene group in

the product **1D** was detected. There was no H/D exchange observed at the position of the bipyridine ring (**Scheme 15**).

A high degree of multiple D incorporation at the *ortho* positions of the N-phenyl ring and the methylene group would suggest that equilibrium might be readily established between the sp^2 and sp^3 C–H bond activation. However, when **1A** was refluxed in AcOD, interestingly, no H/D exchange was detected at the *ortho* position of the phenyl ring whereas a 90% D incorporation into the methylene group was observed (**Scheme 15**, **1E**). These observations suggest that the barrier for the cleavage of the C–Pt bond of **1A** by AcOD may be too high for the reversed process leading to the formation of **1B** to occur. The kinetic barrier for the sp^2 C–H bond activation must be very small so that a rapid equilibrium between **L1** and **1B** can be established and high degree of D scrambling at the *ortho* position of the phenyl ring in the reaction of **L1** and isomerization of **1B** in AcOD could be achieved. The H/D at the methylene group may proceed through a dual agostic interaction, which is illustrated in **Figure 28**.[36]

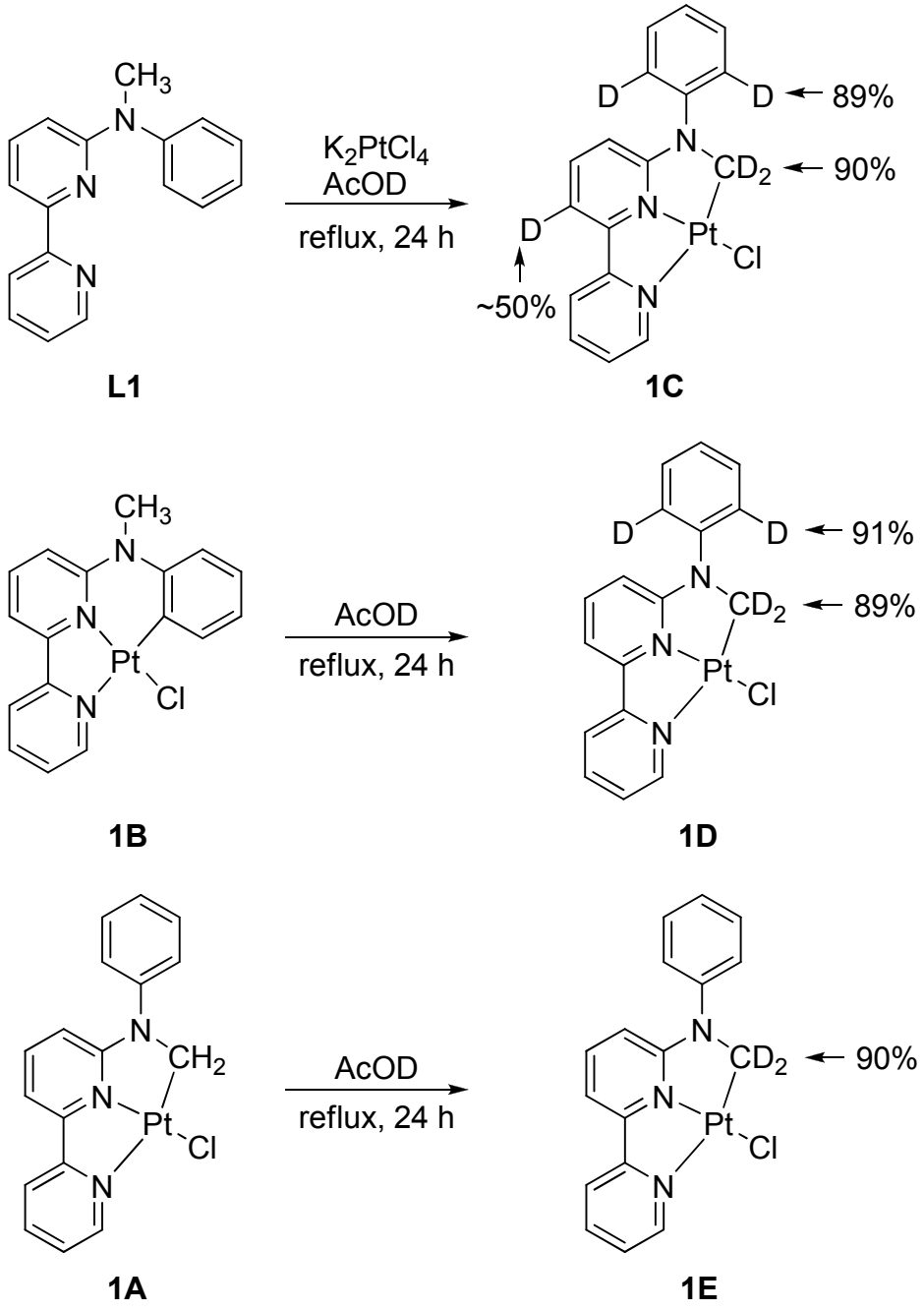

Scheme 15: Reaction, isomerization, and H-D exchange results

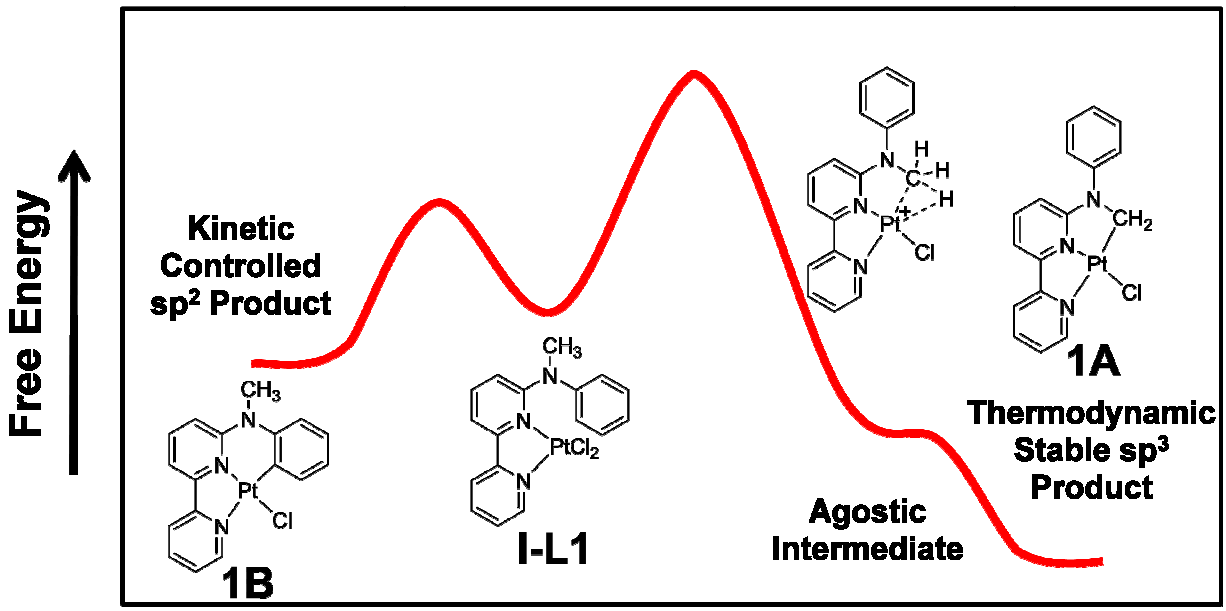

Figure 28: Crude illustration of an energy diagram showing the kinetic and thermodynamic controlled products for each position

To illustrate these energy barriers leading to sp^2 and sp^3 substituted products, a crude energy diagram can be drawn. The bipyridineplatinum complex, intermediate ligand **I-L1**, where the platinum salt has chelated to the nitrogens in the bipyridine in **Figure 28** is considered the starting material for this diagram. When acetonitrile is used as the solvent in the complexation reaction, the kinetically controlled sp^2 product, **1B**, is formed. Acetonitrile is a solvent with a very strong solvent coordinating ability.[48] This characteristic of acetonitrile may deactivate the platinum center toward the more difficult sp^3 C-H bond activation, which gives only the kinetically controlled product exclusively. However, with the increase in the bulk of the N-alkyl group (methyl to ethyl to isopropyl), the steric demand for the reorganization of the ligand for a sp^2 C-H bond activation is increased, the difference in the activation barrier between sp^2 and sp^3 C-H activation is decreased, so the formation of **3A** becomes competitive (**Table 1**).

Solvent Effects

To further explore the solvent effect on the cycloplatination reaction, four reactions were performed using **L1** with K_2PtCl_4 in a mixture of acetonitrile and acetic acid. The results are summarized in **Table 8**. In the reaction with 50% (v/v) of AcOH and acetonitrile as the solvent, the reaction at 90 ^oC for 48 hours gave exclusively the sp^2 C-H bond activation product of **1B**, as determined by the proton NMR spectra of the crude reaction mixture. As the amount of acetic acid is increased, the reactions under the same conditions (90 ^oC, 48h) produced a mixture of **1A** to **1B** with a decreasing ratio of **1B** to **1A**. The reaction was also tested to determine if time was a factor in converting the kinetic controlled product to the thermodynamic product. The 80% acetic acid in acetonitrile experiment was chosen for this study. This reaction was allowed to reflux and was monitored at different time intervals (10, 20, 40, 80 h) by NMR. It was found that the product ration of **1B** to **1A** from 10 to 80 hours was decreased from 69:31 to 5:95 (**Table 9**).

Table 8: The product ratio for the reactions of **L1** with K_2PtCl_4 in mixed solvents at 90 ^oC

AcOH-MeCN (48 h)	
AcOH:MeCN (v/v)	**1B**:**1A**
50:50	100:0
70:30	70:30
80:20	45:55
90:10	26:74

Table 9: The product ratio for the reaction of **L1** at reflux with K_2PtCl_4 at varying times

AcOH:MeCN (v/v, 80:20)	
time (h)	**1B**:**1A**
10	69:31
20	58:42
40	25:75
80	5:95
168	2:98

Results from Mechanistic Studies

All of the results reported in this chapter show that the formation of complex **1B** was kinetically controlled and that the solvent played a crucial role in controlling the chemical kinetics that are involved in this reaction.

CHAPTER 5: SIDE REACTIONS

When performing the various complexation reactions of the three ligands discussed above, there were some side products that resulted from C-C bond cleavage as well as C-N bond cleavage. The ligands that experienced these interesting side reactions were the ethyl ligand (**L2**) and the isopropyl ligand (**L3**). The *tert*-butyl ligand (**L4**) that was shown in **Figure 16**, but never discussed, also underwent C-N bond cleavage; however, there were no desired products obtained from either of the possible isomers, only the two side products.

C-C Bond Cleavage

After the reaction of **L2** with K_2PtCl_4 in AcOH, the formation of a small amount of **1A** (7:93 when compared to **2A**), suggests that the C-C bond of the ethyl group was cleaved (**Scheme 16**). This cleavage is interesting to find due to the fact that the activation of an unstrained C-C single bond is believed to be even more difficult than the C-H bond activation.

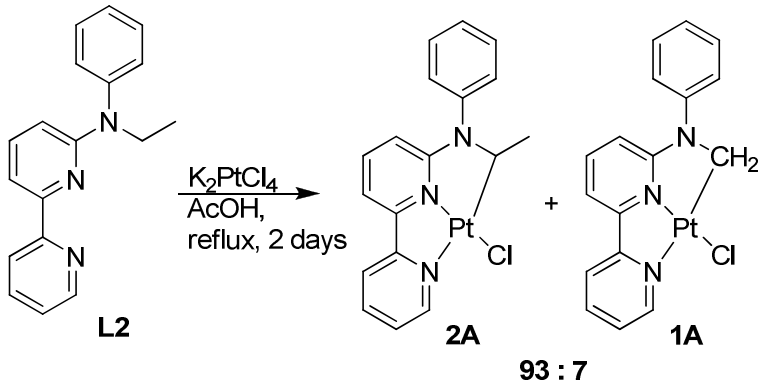

Scheme 16: Reaction of **L2** with K_2PtCl_4 in AcOH to illustrate the side product of **1A**

C-N Bond Cleavage

When the isopropyl ligand (**L3**) was reacted with K_2PtCl_4 in AcOH, an unexpected mixture of products was observed. The major component was one of the predicted isomers (**3A**) while the other two products were neither of the other two possible isomers. Characterizing these side products was very difficult as they had very poor solubility. When the *tert*-butyl ligand (**L4**) was reacted with K_2PtCl_4 in AcOH, none of the desired isomers were produced, only the same two side products from the isopropyl ligand (**Scheme 17**). For this reaction, **3D** was the major product while **3E** was the minor.

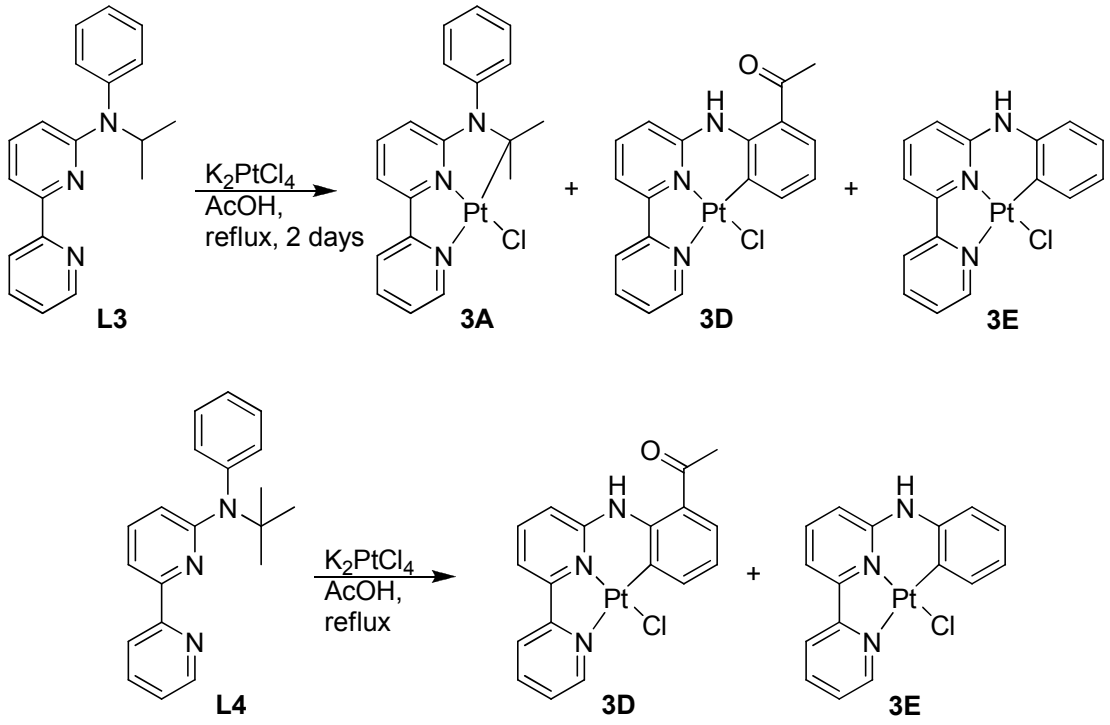

Scheme 17: Reactions of **L3** and **L4** with K_2PtCl_4 in AcOH showing their products

In order to characterize the product, several steps had to be taken. The first step was to obtain the NMR spectra of the side products. The NMR spectrum showed a signal far downfield at 13.93 ppm for the major project, complex **3D**, which would later help in characterizing the structure. After confirming that neither product was a desired isomer, MS^+ was run to obtain the molecular weight of the compounds (MS *m/z* 518(M^+) for **3D** and MS *m/z* 476(M^+) for **3E**). After running the MS experiments, and using this data with the NMR data, the structures of **3D** and **3E** were proposed. X-ray crystal structure determination was the final step in confirming the structure of the complex **3D**. As was stated earlier, these compounds are highly insoluble, and in order to grow a crystal, the compound had to be made more soluble. Substituting the chloride atom for a phenylacetylene group was able to accomplish this (**Scheme 18**). After performing this substitution, a crystal was grown and sent off for X-ray crystal structure determination, the result of which provided some very interesting findings (**Figure 29**). It was found that the peak at 13.9 ppm was actually due to nitrogen's proton that had a very strong hydrogen bond with a carbonyl group from the AcOH that had attached itself to the phenyl ring, causing the peak to show up very far downfield. The bond length from the oxygen to the hydrogen was very small, only 1.8 Å.

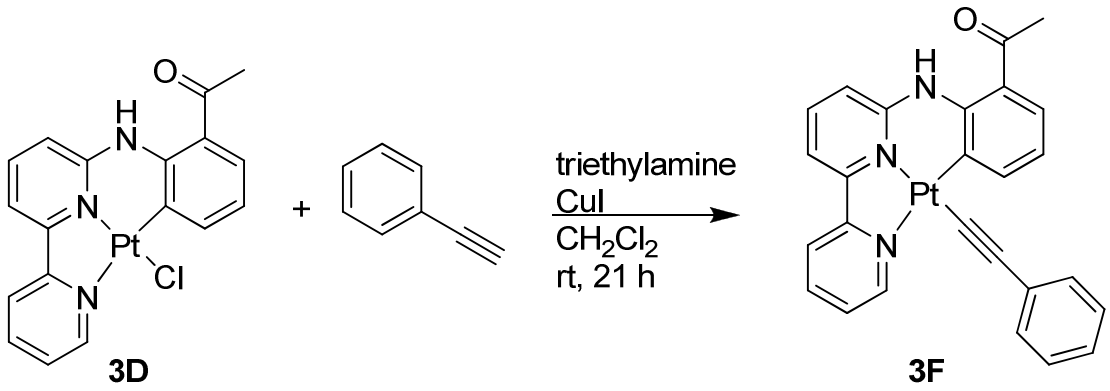

Scheme 18: Reaction of substituting a phenylacetylene for the chloride atom

Whether this hydrogen bonding exists in the process of acylation and plays a role in directing the regioselectivity needs to be further explored.

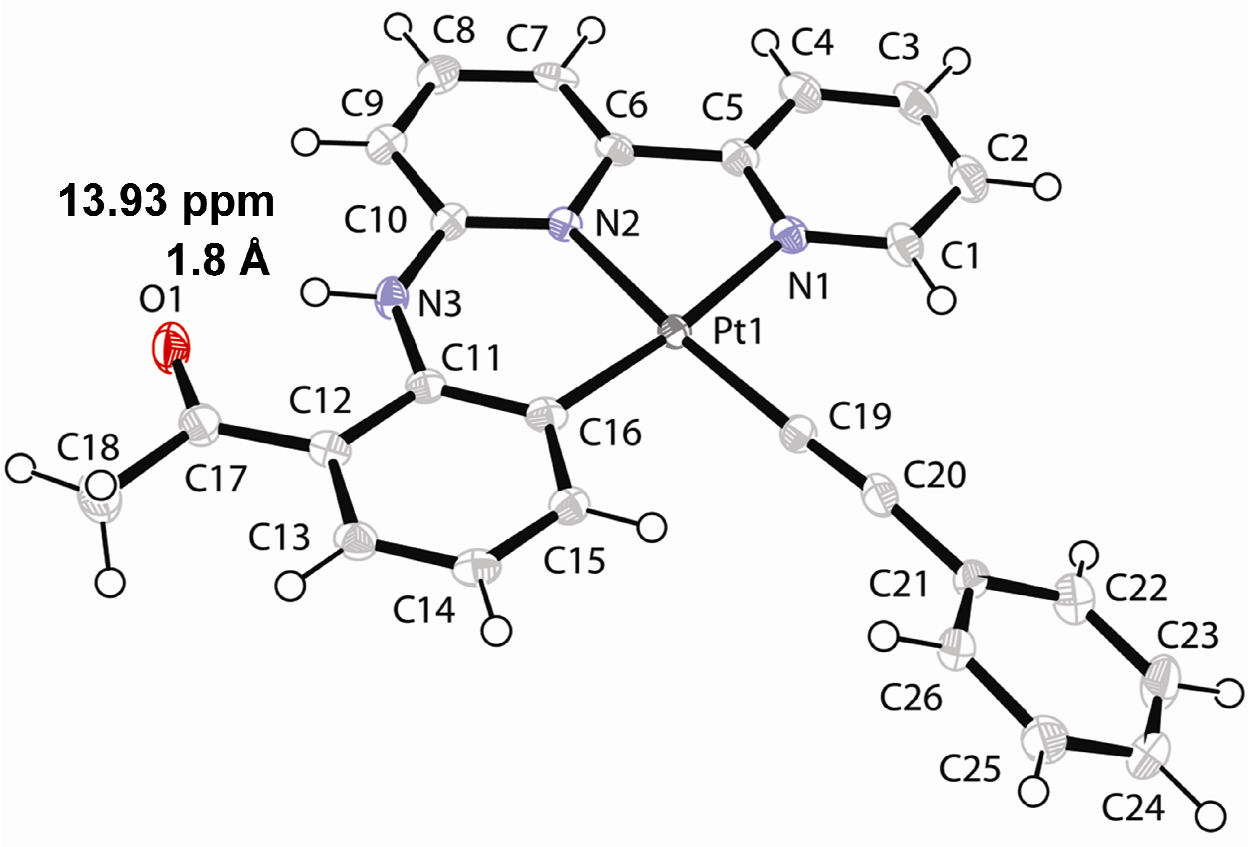

Figure 29: ORTEP diagram of complex **3F**, showing atomic numbering scheme

Table 10: Crystal data and structure refinement for complex **3D**

Identification code	c2onc	
Empirical formula	C26 H19 N3 O Pt, C0.50 H Cl	
Formula weight	627.00	
Temperature	100(2) K	
Wavelength	1.54178 Å	
Crystal system	Monoclinic	
Space group	C2/c	
Unit cell dimensions	a = 31.5338(6) Å	a= 90°.
	b = 8.0506(2) Å	b= 112.2730(10)°.
	c = 19.1014(4) Å	g = 90°.
Volume	4487.39(17) $Å^3$	
Z	8	
Density (calculated)	1.856 Mg/m^3	
Absorption coefficient	12.989 mm^{-1}	
F(000)	2424	
Crystal size	0.34 x 0.33 x 0.21 mm^3	
Theta range for data collection	4.77 to 66.98°.	
Index ranges	-37<=h<=36, -9<=k<=9, -22<=l<=22	
Reflections collected	23539	
Independent reflections	3980 [R(int) = 0.0457]	
Completeness to theta = 66.98°	99.3 %	
Absorption correction	Numerical	
Max. and min. transmission	0.1694 and 0.0969	
Refinement method	Full-matrix least-squares on F^2	
Data / restraints / parameters	3980 / 0 / 295	
Goodness-of-fit on F^2	1.098	
Final R indices [I>2sigma(I)]	R1 = 0.0274, wR2 = 0.0728	
R indices (all data)	R1 = 0.0278, wR2 = 0.0730	
Largest diff. peak and hole	1.868 and -1.321 $e.Å^{-3}$	

Table 11: Atomic coordinates (x 10^4) and equivalent isotropic displacement parameters ($Å^2$x 10^3) for complex **3D** U(eq) is defined as one third of the trace of the orthogonalized U^{ij} tensor

	x	y	z	U(eq)
Pt(1)	2110(1)	5956(1)	4133(1)	14(1)
O(1)	3982(1)	6862(4)	4476(2)	30(1)
N(1)	1772(1)	4746(4)	4737(2)	19(1)
N(2)	2654(1)	5066(4)	5018(2)	14(1)
N(3)	3222(1)	6152(4)	4629(2)	19(1)
C(1)	1317(1)	4678(5)	4556(3)	23(1)
C(2)	1126(2)	3829(6)	4995(3)	29(1)
C(3)	1411(2)	3011(6)	5634(3)	29(1)
C(4)	1881(2)	3076(5)	5827(3)	24(1)
C(5)	2054(2)	3973(5)	5372(3)	20(1)
C(6)	2549(2)	4136(5)	5542(2)	18(1)
C(7)	2878(2)	3460(5)	6164(2)	21(1)
C(8)	3340(2)	3715(6)	6280(3)	23(1)
C(9)	3448(1)	4645(5)	5777(2)	21(1)
C(10)	3097(1)	5301(5)	5135(2)	17(1)
C(11)	2979(1)	7014(5)	3967(2)	17(1)
C(12)	3254(1)	7809(5)	3613(2)	20(1)
C(13)	3037(2)	8772(5)	2970(2)	21(1)
C(14)	2569(2)	8953(5)	2679(2)	22(1)
C(15)	2305(1)	8125(5)	3010(2)	18(1)
C(16)	2495(1)	7117(5)	3656(2)	18(1)
C(17)	3761(2)	7667(6)	3904(2)	24(1)
C(18)	4023(2)	8535(7)	3502(3)	33(1)
C(19)	1540(1)	6633(5)	3311(2)	18(1)
C(20)	1181(1)	6980(5)	2827(2)	21(1)
C(21)	770(1)	7470(5)	2192(2)	20(1)
C(22)	364(2)	6571(6)	2000(3)	29(1)
C(23)	-20(2)	7007(7)	1382(3)	36(1)
C(24)	-9(2)	8341(7)	930(3)	35(1)

C(25)	387(2)	9254(7)	1103(3)	32(1)
C(26)	775(2)	8819(6)	1739(3)	24(1)
Cl(1)	406(1)	2198(2)	3193(1)	49(1)
C(27)	0	954(8)	2500	31(2)

Table 12: Bond lengths [Å] and angles [°] for **3D**

Pt(1)-C(19)	1.961(4)
Pt(1)-C(16)	2.006(4)
Pt(1)-N(2)	2.029(3)
Pt(1)-N(1)	2.084(3)
O(1)-C(17)	1.234(6)
N(1)-C(1)	1.343(5)
N(1)-C(5)	1.353(6)
N(2)-C(10)	1.341(5)
N(2)-C(6)	1.388(5)
N(3)-C(10)	1.360(5)
N(3)-C(11)	1.391(5)
N(3)-H(3N)	0.8800
C(1)-C(2)	1.383(7)
C(1)-H(1)	0.9500
C(2)-C(3)	1.378(7)
C(2)-H(2)	0.9500
C(3)-C(4)	1.386(6)
C(3)-H(3)	0.9500
C(4)-C(5)	1.391(6)
C(4)-H(4)	0.9500
C(5)-C(6)	1.474(6)
C(6)-C(7)	1.360(6)
C(7)-C(8)	1.402(6)
C(7)-H(7)	0.9500
C(8)-C(9)	1.362(6)
C(8)-H(8)	0.9500
C(9)-C(10)	1.407(6)
C(9)-H(9)	0.9500
C(11)-C(16)	1.412(6)
C(11)-C(12)	1.437(6)
C(12)-C(13)	1.393(6)
C(12)-C(17)	1.486(6)

C(13)-C(14)	1.375(7)
C(13)-H(13)	0.9500
C(14)-C(15)	1.390(6)
C(14)-H(14)	0.9500
C(15)-C(16)	1.408(6)
C(15)-H(15)	0.9500
C(17)-C(18)	1.497(6)
C(18)-H(18A)	0.9800
C(18)-H(18B)	0.9800
C(18)-H(18C)	0.9800
C(19)-C(20)	1.192(6)
C(20)-C(21)	1.455(6)
C(21)-C(26)	1.392(6)
C(21)-C(22)	1.395(6)
C(22)-C(23)	1.379(7)
C(22)-H(22)	0.9500
C(23)-C(24)	1.387(8)
C(23)-H(23)	0.9500
C(24)-C(25)	1.378(7)
C(24)-H(24)	0.9500
C(25)-C(26)	1.402(7)
C(25)-H(25)	0.9500
C(26)-H(26)	0.9500
Cl(1)-C(27)	1.764(4)
C(27)-Cl(1)#1	1.764(4)
C(27)-H(27A)	0.9900
C(27)-H(27B)	0.9900

C(19)-Pt(1)-C(16)	92.08(16)
C(19)-Pt(1)-N(2)	173.38(15)
C(16)-Pt(1)-N(2)	94.32(14)
C(19)-Pt(1)-N(1)	93.89(15)
C(16)-Pt(1)-N(1)	173.76(14)
N(2)-Pt(1)-N(1)	79.77(13)

C(1)-N(1)-C(5)	119.1(4)
C(1)-N(1)-Pt(1)	126.6(3)
C(5)-N(1)-Pt(1)	114.3(3)
C(10)-N(2)-C(6)	118.3(3)
C(10)-N(2)-Pt(1)	126.0(3)
C(6)-N(2)-Pt(1)	115.7(3)
C(10)-N(3)-C(11)	133.6(4)
C(10)-N(3)-H(3N)	113.2
C(11)-N(3)-H(3N)	113.2
N(1)-C(1)-C(2)	122.1(4)
N(1)-C(1)-H(1)	118.9
C(2)-C(1)-H(1)	118.9
C(3)-C(2)-C(1)	119.1(4)
C(3)-C(2)-H(2)	120.4
C(1)-C(2)-H(2)	120.4
C(2)-C(3)-C(4)	119.3(4)
C(2)-C(3)-H(3)	120.4
C(4)-C(3)-H(3)	120.4
C(5)-C(4)-C(3)	119.1(4)
C(5)-C(4)-H(4)	120.4
C(3)-C(4)-H(4)	120.4
N(1)-C(5)-C(4)	121.3(4)
N(1)-C(5)-C(6)	115.9(4)
C(4)-C(5)-C(6)	122.8(4)
C(7)-C(6)-N(2)	122.2(4)
C(7)-C(6)-C(5)	123.5(4)
N(2)-C(6)-C(5)	114.3(4)
C(6)-C(7)-C(8)	118.9(4)
C(6)-C(7)-H(7)	120.6
C(8)-C(7)-H(7)	120.6
C(9)-C(8)-C(7)	119.5(4)
C(9)-C(8)-H(8)	120.2
C(7)-C(8)-H(8)	120.2
C(8)-C(9)-C(10)	119.7(4)

C(8)-C(9)-H(9)	120.1
C(10)-C(9)-H(9)	120.1
N(2)-C(10)-N(3)	121.1(3)
N(2)-C(10)-C(9)	121.3(4)
N(3)-C(10)-C(9)	117.6(4)
N(3)-C(11)-C(16)	123.1(4)
N(3)-C(11)-C(12)	115.3(4)
C(16)-C(11)-C(12)	121.6(4)
C(13)-C(12)-C(11)	118.7(4)
C(13)-C(12)-C(17)	118.1(4)
C(11)-C(12)-C(17)	123.1(4)
C(14)-C(13)-C(12)	120.6(4)
C(14)-C(13)-H(13)	119.7
C(12)-C(13)-H(13)	119.7
C(13)-C(14)-C(15)	120.0(4)
C(13)-C(14)-H(14)	120.0
C(15)-C(14)-H(14)	120.0
C(14)-C(15)-C(16)	123.1(4)
C(14)-C(15)-H(15)	118.4
C(16)-C(15)-H(15)	118.4
C(15)-C(16)-C(11)	115.8(4)
C(15)-C(16)-Pt(1)	122.5(3)
C(11)-C(16)-Pt(1)	121.7(3)
O(1)-C(17)-C(12)	122.5(4)
O(1)-C(17)-C(18)	117.6(4)
C(12)-C(17)-C(18)	119.8(4)
C(17)-C(18)-H(18A)	109.5
C(17)-C(18)-H(18B)	109.5
H(18A)-C(18)-H(18B)	109.5
C(17)-C(18)-H(18C)	109.5
H(18A)-C(18)-H(18C)	109.5
H(18B)-C(18)-H(18C)	109.5
C(20)-C(19)-Pt(1)	176.3(4)
C(19)-C(20)-C(21)	174.1(4)

C(26)-C(21)-C(22)	117.8(4)
C(26)-C(21)-C(20)	120.9(4)
C(22)-C(21)-C(20)	121.2(4)
C(23)-C(22)-C(21)	120.9(5)
C(23)-C(22)-H(22)	119.5
C(21)-C(22)-H(22)	119.5
C(22)-C(23)-C(24)	120.6(4)
C(22)-C(23)-H(23)	119.7
C(24)-C(23)-H(23)	119.7
C(25)-C(24)-C(23)	119.9(4)
C(25)-C(24)-H(24)	120.1
C(23)-C(24)-H(24)	120.1
C(24)-C(25)-C(26)	119.3(5)
C(24)-C(25)-H(25)	120.4
C(26)-C(25)-H(25)	120.4
C(21)-C(26)-C(25)	121.5(4)
C(21)-C(26)-H(26)	119.3
C(25)-C(26)-H(26)	119.3
Cl(1)-C(27)-Cl(1)#1	110.8(4)
Cl(1)-C(27)-H(27A)	109.5
Cl(1)#1-C(27)-H(27A)	109.5
Cl(1)-C(27)-H(27B)	109.5
Cl(1)#1-C(27)-H(27B)	109.5
H(27A)-C(27)-H(27B)	108.1

CHAPTER 6: CONCLUSIONS

Through this research, it has been demonstrated that selective formation of cyclometalated platinum complexes through either the sp^2 or the sp^3 C-H bond activation can be readily achieved by simply switching the solvent in which the reaction is performed. This remarkable solvent-controlled switch of selectivity not only offers an excellent method to control the product formation but also provides an interesting system for probing some important mechanistic issues associated with the transition metal-assisted C-H bond activations. It was determined that the products formed from a complexation reaction in acetonitrile were kinetically controlled while those formed from a complexation reaction in glacial acetic acid were thermodynamically controlled. Based on the solvent studies, it was found that the ratio of products also depends on time, where as more time goes by the thermodynamically stable product begins to predominate. Beyond this, several side reactions due to C-C and C-N bond cleavage were also uncovered and the products characterized, which will open the door to future mechanistic studies related to the cycloplatination.

CHAPTER 7: EXPERIMENTAL

Synthesis

General:

All manipulations were conducted under a dry nitrogen atmosphere and anhydrous conditions. Tetrahydrofuran (THF) was distilled from sodium and benzophenone. All other anhydrous solvents used were purchased from Sigma-Aldrich with Sure Seal. All catalysts and reagents were purchased from Sigma-Aldrich, with the exception of K_2PtCl_4 which was purchased from Strem Chemicals. Commercial reagent grade solvents and chemicals were used as obtained unless otherwise noted. 6-Bromo-2,2'-bipyridine was prepared following the literature procedure.[49] Preparative chromatography was performed on silica gel 60 (0.063-0.200 mm) purchased from EMD chemicals. Thin layer chromatography was performed with silica gel 60 F_{254} plates, purchased from EMD chemicals. ^{1}H and ^{13}C NMR spectra were recorded on Varian 500 MHz and 300 MHz spectrometers at 298K. Chemical shifts were reported relative to TMS (0.0 ppm for ^{1}H), dichloromethane-d_2 (53.8 ppm for ^{13}C), chloroform-d (77.0 ppm for ^{13}C), DMSO-d_6 (39.5 ppm for ^{13}C) and coupling constants are in Hertz. Elemental analyses were performed in Analytical Microlabs, Norcross, GA.

Preparation of the Ligands L1, L2, and L3

*N-Methyl-N-phenyl-2,2'-bipyridin-6-amine (**L1)***

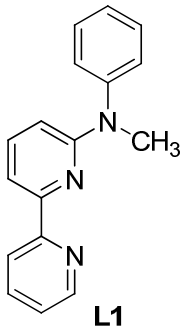

L1

General Procedure A: To a 50 mL dry, three necked flask were added N-methylaniline (0.16 mL, 1.5 mmol), 6-bromo-2,2'-bipyridine (235 mg, 1.0 mmol), $Pd(dba)_2$ (23 mg, 0.04 mmol), DPPF (22 mg, 0.04 mmol), sodium *tert*-butoxide (115 mg, 1.2 mmol), and toluene (15 mL). The reaction mixture was refluxed under nitrogen for 1 hour. After cooling to room temperature, the reaction mixture was quenched with water and extracted with ethyl acetate (3 x 50 mL). The combined organic phases were washed with water (50 mL), brine (50 mL), dried over $MgSO_4$, filtered, and evaporated. The crude product was purified by column chromatography on silica gel with dichloromethane and ethyl acetate (v/v: 40:1 to 20:1) to give a white colored solid, 206 mg, 79%. ^{1}H NMR (500 MHz, $CDCl_3$) δ 8.65 (d, J = 4.5 Hz, 1H), 8.43 (d, J = 9.0 Hz, 1H), 7.79-7.76 (m, 2H), 7.47-7.39 (m, 3H), 7.32-7.30 (m, 2H), 7.27-7.20 (m, 2H), 6.59 (d, J = 9.0 Hz, 1H), 3.60 (s, 3H). ^{13}C NMR (75 MHz, $CDCl_3$) δ 158.2, 156.9, 153.8, 148.9, 146.9, 137.5, 136.6, 129.6 (2C), 126.3 (2C), 125.3, 123.2, 120.9, 110.4, 109.4, 38.2. Anal. Calcd for $C_{17}H_{15}N_3$: C, 78.13; H, 5.79; N, 16.08. Found: C, 77.93; H, 5.70; N, 15.95.

*N-Ethyl-N-phenyl-2,2'-bipyridin-6-amine (**L2)***

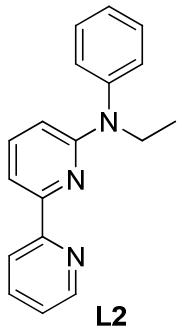

L2

This compound was prepared according to the **General Procedure A**. The crude product was purified by column chromatography on silica gel with dichloromethane and ethyl acetate (v/v: 3:1) then hexane and ethyl acetate (v/v: 5:1) to give a light yellow colored solid, yield 89%. ^{1}H NMR (500 MHz, $CDCl_3$) δ 8.65 (d, *J* = 4.5 Hz, 1H), 8.42 (d, *J* = 8.5 Hz, 1H), 7.80 (dt, *J* = 7.8, 2.0Hz, 1H), 7.74 (d, *J* = 7.0 Hz, 1H), 7.44-7.40 (m, 3H), 7.30-7.24 (m, 4H), 6.42 (d, *J* = 8.5 Hz, 1H), 4.15 (q, *J* = 7.0 Hz, 2H), 1.31 (t, *J* = 7.0 Hz, 3H). ^{13}C NMR (75 MHz, $CDCl_3$) δ 157.9, 157.2, 153.8, 149.0, 145.7, 137.7, 136.9, 129.9 (2C), 127.9 (2C), 126.0, 123.4, 121.1, 110.3, 109.8, 45.3, 13.3. Anal. Calcd for $C_{18}H_{17}N_3$: C, 78.52; H, 6.22; N, 15.26. Found: C, 78.24; H, 6.18; N, 15.31.

*N-Isopropyl-N-phenyl-2,2'-bipyridin-6-amine (**L3)***

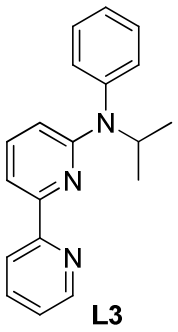

L3

This compound was prepared according to the **General Procedure A**. The crude product was purified by column chromatography on silica gel with a mixture of dichloromethane and hexane (v/v: 1:1) to give a white solid, yield 55%. **^{1}H NMR** (500 MHz, $CDCl_3$) δ 8.65 (d, *J* = 4.5 Hz, 1H), 8.44 (d, *J* = 9.5 Hz, 1H), 7.81 (dt, *J* = 8.0, 2.0 Hz, 1H), 7.69 (d, *J* = 7.5 Hz, 1H), 7.46 (t, *J* = 7.5 Hz, 2H), 7.38-7.33 (m, 2H), 7.28-7.25 (m, 1H), 7.21-7.19 (m, 2H), 6.00 (d, *J* = 8.0 Hz, 1H), 5.47-5.39 (m, 1H), 1.22 (d, *J* = 7 Hz, 6H). **^{13}C NMR** (75 MHz, $CDCl_3$) δ 158.4, 157.1, 153.2, 148.7, 141.5, 137.4, 136.8, 131.5 (2C), 129.6 (2C), 127.2, 123.1, 120.9, 109.7, 109.4, 46.4, 21.1 (2C). Anal. Calcd for $C_{19}H_{19}N_3$: C, 78.86; H, 6.62; N, 14.52. Found: C, 78.59; H, 6.55; N, 14.42.

Reaction of L1, L2, and L3 with K_2PtCl_4

*Complex **1B***

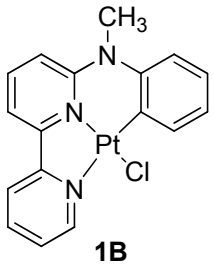

1B

To a dry 50 mL three necked flask were added **L1** (118 mg, 0.45 mmol), K_2PtCl_4 (187 mg, 0.45 mmol), and acetonitrile (20 mL). The reaction mixture was refluxed for 3 days then cooled to room temperature. The solvent was removed by a rotavapor, and the crude product was purified by column chromatography on silica gel with a mixture of dichloromethane and ethyl acetate (v/v: 50:1, 25:1) to give an orange solid (**1a**), 161 mg, 73%. ^{1}H NMR (500 MHz, $CDCl_3$) δ 9.78 (d, *J* = 5.0 Hz, 1H), 8.44 (dd, *J* = 7.5, 1.5 Hz, $^{3}J_{Pt\text{-}H}$ = 27.3 Hz, 1H), 8.04-8.00 (m,

2H), 7.95 (t, *J* = 8.5 Hz, 1H), 7.60 (dt, *J* = 6.0, 2.5 Hz, 1H), 7.51 (d, J = 7.5 Hz, 1H), 7.22-7.18 (m, 1H), 7.14-7.11 (m, 1H), 7.08 (d, *J* = 8.0 Hz, 1H), 6.98 (t, *J* = 7.0 Hz, 1H), 3.74 (s, 3H). ^{13}C NMR (75 MHz, CD_2Cl_2) δ 156.5, 155.1, 151.6, 148.5, 141.0, 139.5, 138.5, 136.5, 126.2, 124.4, 122.3, 122.0, 119.0, 116.9, 115.5, 114.7 (J_{Pt-C} = 14.6 Hz), 42.3. Anal. Calcd for $C_{17}H_{14}ClN_3Pt$: C, 41.60; H, 2.87; N, 8.56. Found: C, 41.70; H, 2.78; N, 8.63.

*Complex **1A***

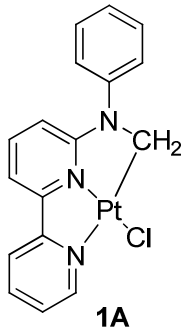

1A

To a dry 50 mL three necked flask were added **L1** (117 mg, 0.45 mmol), K_2PtCl_4 (186 mg, 0.45 mmol), and glacial acetic acid (20 mL). The reaction mixture was refluxed for 24h then cooled to room temperature. The solvent was removed by a rotavapor and the crude product was purified by column chromatography on silica gel with a mixture of dichloromethane and ethyl acetate (v/v: 10:1) to give an orange solid that contains small amount of **1a**. The solid was dissolved in dichloromethane and pure **1b** was precipitated by addition of methanol, 160 mg, 73%. ^{1}H NMR (500 MHz, CD_2Cl_2) δ 9.10 (dd, *J* = 5.5, 1.0 Hz, 1H), 8.10 (dt, *J* = 8.0, 1.5 Hz, 1H), 7.99 (d, *J* = 8.0 Hz, 1H), 7.68-7.65 (m, 1H), 7.60 (t, *J* = 8.3 Hz, 1H), 7.49-7.45 (m, 2H), 7.40-7.38 (m, 2H), 7.33 (t, *J* = 7.5 Hz, 1H), 7.13 (d, *J* = 8.0 Hz, 1H) 6.51 (d, *J* = 9.0 Hz, 1H), 5.42 (s, $^2J_{Pt-H}$ = 40.5 Hz, 2H). ^{13}C NMR (75 MHz, CD_2Cl_2) δ 159.8, 157.3, 151.5, 147.9, 144.1,

138.5, 135.9, 130.2 (2C), 127.2, 127.1, 125.5 (2C), 122.2, 111.1, 110.0, 36.4 (J_{Pt-C} = 416.2 Hz). Anal. Calcd for $C_{17}H_{14}ClN_3Pt$: C, 41.60; H, 2.87; N, 8.56. Found: C, 41.35; H, 2.79; N, 8.47.

*Complex **2B***

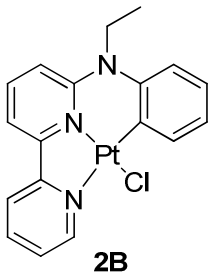

2B

To a dry 50 mL three necked flask were added **L2** (137 mg, 0.5 mmol), K_2PtCl_4 (208 mg, 0.5 mmol), and acetonitrile (20 mL). The reaction mixture was refluxed for 2 days then cooled to room temperature. The solvent was removed by rotavapor and the crude product was purified by column chromatography on silica gel with a mixture of dichloromethane and ethyl acetate (v/v=100:1) to give an orange solid, 174 mg. Further purification was done by dissolving the solid in dichloromethane followed by the addition of methanol, The precipitates were collected and dried in air, 164 mg, 70%. ^{1}H NMR (500 MHz, $CDCl_3$) δ 9.79 (d, J = 4.5 Hz, 1H), 8.43 (d, J = 8.0 Hz, $^3J_{Pt-H}$ = 27.3 Hz, 1H), 8.05-8.00 (m, 2H), 7.93 (t, J = 8.0 Hz, 1H), 7.62-7.59 (m, 1H), 7.51 (d, J = 7.5 Hz, 1H), 7.30 (d, J = 9.0 Hz, 1H), 7.15-7.08 (m, 2H), 6.98 (t, J = 8.0 Hz, 1H), 4.25 (q, J = 7.0 Hz, 2H), 1.44 (t, J = 6.5 Hz, 3H). ^{13}C NMR (75 MHz, DMSO-d_6) δ 155.7, 154.1, 150.5, 147.2, 139.3, 139.1, 138.9, 137.0, 126.4, 123.7, 122.9, 120.9, 119.9, 118.4, 116.4, 115.7, 47.5, 14.1. Anal. Calcd for $C_{18}H_{16}ClN_3Pt$: C, 42.82; H, 3.19; N, 8.32. Found: C, 42.33; H, 2.97; N, 8.17.

*Complex **2A***

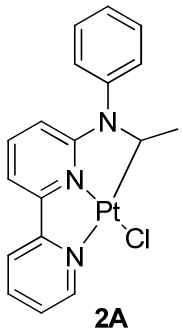

2A

To a dry 50 mL three necked flask were added **L2** (180.0 mg, 0.65 mmol), K_2PtCl_4 (270 mg, 0.6 mmol), and glacial acetic acid (20 mL). The reaction mixture was refluxed for 2 days then cooled to room temperature. It was then quenched by water and extracted with dichloromethane (3 x 75 mL). The combined organic phases were washed with water (100 mL), brine (100 mL), dried over $MgSO_4$, and filtered. The solvents were removed by rotavapor and the crude product was purified by column chromatography on silica gel with a mixture of dichloromethane and ethyl acetate (v/v: 25:1) to give an orange solid, which was further purified by recrystallization from CH_2Cl_2-methanol, 224 mg, 63%. ^{1}H NMR (500 MHz, $CDCl_3$) δ 9.19 (d, *J* = 6.0 Hz, 1H), 8.05 (dt, *J* = 8.0, 1.5 Hz, 1H), 7.93 (d, *J* = 8.0 Hz, 1H), 7.62-7.60 (m, 1H), 7.54-7.47 (m, 3H), 7.38-7.35 (m, 1H), 7.30-7.28 (m, 2H), 7.06 (d, *J* = 8.0 Hz, 1H), 6.29 (d, *J* = 9.0 Hz, 1H), 5.88 (q, *J* = 7.0 Hz, $^2J_{Pt\text{-}C}$ = 48.0 Hz, 1H), 1.40 (d, *J* = 7.0 Hz, $^3J_{Pt\text{-}H}$ 21.5 Hz, 3H). ^{13}C NMR (75 MHz, CD_2Cl_2) δ 160.2, 157.2, 151.2, 148.3, 140.8, 138.5, 135.9, 134.3, 130.2, 127.9, 127.7, 126.9, 125.5, 122.1, 110.3, 109.7, 46.3 ($J_{Pt\text{-}C}$ = 436.9 Hz), 23.8. Anal. Calcd for $C_{18}H_{16}ClN_3Pt$•0.5 CH_2Cl_2: C, 41.17; H, 3.27; N, 7.58. Found: C, 40.76; H, 3.11; N, 7.68.

*Complex **3B***

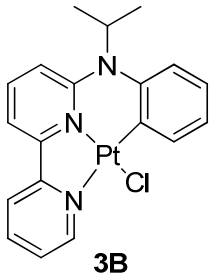

3B

To a dry 50 mL three necked flask were added **L3** (145 mg, 0.50 mmol), K_2PtCl_4 (214 mg, 0.51 mmol) and acetonitrile (20 mL). The reaction mixture was refluxed for 4 days then cooled to room temperature. The solvent was removed by rotavapor and the crude product was purified by column chromatography on silica gel with a mixture of dichloromethane and ethyl acetate (v/v=50:1) to give an orange solid that contains both **3a** and **3b**. Further purification by recrystallization from dichloromethane and hexane to give 97 mg pure **3a** as orange crystals, 36% yield. ^{1}H NMR (500 MHz, $CDCl_3$) δ 9.64 (1H, d, *J* = 5.0 Hz), 8.20 (d, *J* = 7.5 Hz, $^3J_{Pt\text{-}H}$ 25.3 Hz, 1H), 8.06-8.02 (m, 2H), 7.95-7.92 (m, 1H), 7.63-7.56 (m, 2H), 7.46 (d, *J* = 8.0 Hz, 1H), 7.27 (d, *J* = 8.0 Hz, 1H), 7.05-7.02 (m, 1H), 6.90 (td, *J* = 1.5, 7.3 Hz, 1H), 4.43-4.34 (m, 1H), 1.61 (d, *J* = 6.5 Hz, 6H). ^{13}C NMR (75 MHz, CD_2Cl_2) δ 156.8, 155.4, 153.9, 148.3, 140.4, 139.3, 138.5, 136.3, 126.2, 123.9, 122.8, 122.1, 119.8, 119.2, 115.7, 114.6, 58.8, 23.7 (2C). Anal. Calcd for $C_{19}H_{18}ClN_3Pt$: C, 43.98; H, 3.50; N, 8.10. Found: C, 43.93; H, 3.43; N, 8.22.

*Complex **3A***

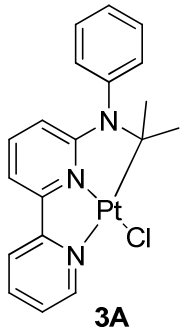

3A

To a dry 50 mL three necked flask were added **L3** (145 mg, 0.50 mmol), K_2PtCl_4 (210 mg, 0.51 mmol) and acetonitrile (20 mL). The reaction mixture was refluxed for 2 days then cooled to room temperature. The solvent was removed by rotavapor and the crude product was purified by column chromatography on silica gel with a mixture of dichloromethane and ethyl acetate (v/v=15:1) to give an orange solid, 99 mg, 38% yield. ^{1}H NMR (500 MHz, $CDCl_3$) δ 9.09 (d, *J* = 5.5 Hz, 1H), 8.06 (td, *J* = 1.5, 8.0 Hz, 1H), 7.95 (d, *J* = 7.0 Hz, 1H), 7.62-7.60 (m, 1H), 7.53-7.46 (m, 4H), 7.22-7.20 (m, 2H), 7.08 (d, *J* = 7.0 Hz, 1H), 5.91 (d, *J* = 8.5, 1H), 1.49 (s, $^3J_{Pt-H}$ = 17.5 Hz, 6H). ^{13}C NMR (75 MHz, CD_2Cl_2) δ 160.8, 157.1, 150.7, 148.5, 138.5, 137.0, 135.9, 131.2 (2C), 130.2 (2C), 128.5, 126.8, 122.1, 110.0, 109.2, 55.3 (J_{Pt-C} = 458.7 Hz), (2C) 31.6. Anal. Calcd for $C_{19}H_{18}ClN_3Pt$: C, 43.98; H, 3.50; N, 8.10. Found: C, 44.07; H, 3.34; N, 8.10.

Reaction of L1 with K_2PtCl_4 in AcOD

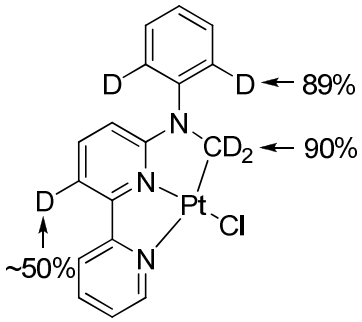

1c

To a dry 50 mL three necked flask were added **L1** (131 mg, 0.50 mmol), K_2PtCl_4 (208 mg, 0.50 mmol), and deuterated glacial acetic acid (20 mL). The reaction mixture was refluxed for 24 h then cooled to room temperature. The solvent was removed by a rotavapor, and the crude product analyzed by NMR to determine the level of H/D exchange. ^{1}H NMR of **1c** (500 MHz, $CDCl_3$) δ 9.20 (d, *J* = 4.0 Hz, 1H), 8.08 (t, *J* = 7.8 Hz, 1H), 7.95 (d, *J* = 8.0 Hz, 1H), 7.67-7.64 (m, 1H), 7.58-7.55 (m, this proton is partially deuterated with ~50% deuteration), 7.47-7.45 (m, 2H), 7.33 (t, *J* = 7.0 Hz, 1H), 7.07 (d, *J* = 7.0 Hz, 1H), 6.51 (d, *J* = 9.0 Hz, 1H).

Isomerization of 1A in AcOD

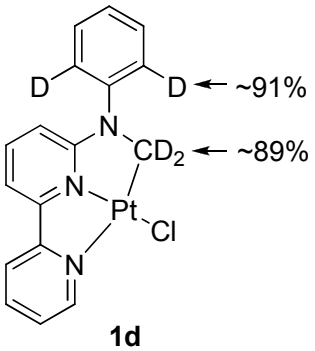

1d

To a dry 50 mL flask were added 11.2 mg of **1a** and deuterated glacial acetic acid (4.0 mL). The reaction was refluxed for 3 days then cooled to room temperature. The solvent was removed by rotavapor and the crude product analyzed by NMR to determine the level of H/D exchange. ^{1}H NMR of **1d** (500 MHz, $CDCl_3$) δ (ppm): 9.21 (d, *J* = 5.3 Hz, 1H), 8.07 (t, *J* = 8.0 Hz, 1H), 7.94 (d, *J* = 8.5 Hz, 1H), 7.67-7.64 (m, 1H), 7.58-7.54 (m, 1H), *7*.45 (d, *J* = 7.0 Hz, 2H), 7.32 (t, *J* = 7.0 Hz, 1H), 7.06 (d, *J* = 7.0 Hz, 1H), 6.50 (d, *J* = 9.0 Hz, 1H).

Reaction of L1 with K_2PtCl_4 in Mixed Solvents

AcOH-MeCN (v/v 50:50)

To a dry 25 mL three necked flask were added **L1** (32.0 mg, 0.12 mmol), K_2PtCl_4 (51 mg, 0.12 mmol), glacial acetic acid (4.0 mL), and acetonitrile (4.0 mL). The reaction mixture was heated to 90 ^{o}C for 48 h then cooled to room temperature. Aqueous workup performed by diluting the mixture with dichloromethane and washing with distilled water (3 x 20 mL). The organic phase was dried over $MgSO_4$, filtered, and the solvent removed by rotavapor. The crude product was then examined by NMR and the ratio of **1a** to **1b** was determined to be 100:0.

AcOH-MeCN (v/v 70:30)

The reaction was carried out using the same procedure described above except for the solvents (AcOH-MeCN, v/v 70:30; 90 ^{o}C for 48 h). The crude product was then examined by NMR and the ratio of **1a** to **1b** was determined to be 70:30.

AcOH-MeCN (v/v 80:20)

The reaction was carried out using the same procedure described above except for the solvents (AcOH-MeCN, v/v 80:20; 90 ^{o}C for 48 h). This reaction was performed again with the same ratio of solvent but heated to reflux and the reaction mixture was taken periodically (10, 20,

40, 80, and 160 h) for NMR analysis and the ratio of **1a** to **1b** was determined to be 69:31, 58:42, 25:75, 5:95, and 2:98, respectively.

AcOH-MeCN (v/v 90:10)

The reaction was carried out using the same procedure described above except for the solvents (AcOH-MeCN, v/v 90:10; 90 ^{o}C, 48 h). The crude product was then examined by NMR and the ratio of **1a** to **1b** was determined to be 16:84.

X-Ray Crystallography:

Crystals were grown by solvent diffusion method, by diffusing hexane into a solution of dichloromethane. A red plate crystal was selected and mounted on a glass fiber. All measurements were made using graphite-monochromated Cu Ka radiation on a Bruker-AXS three-circle diffractometer, equipped with a SMART Apex II CCD detector. Initial space group determination was based on a matrix consisting of 120 frames. The data was reduced using SAINT+[50], and empirical absorption correction applied using SADABS.[51] Structures were solved using direct methods. Least-squares refinement for all structures was carried out on F^2. The non-hydrogen atoms were refined anisotropically. Hydrogen atoms were placed in calculated positions and allowed to refine isotropically as riding models. Structure solution, refinement and the calculation of derived results were performed using the SHELXTL package of computer programs.[52] Details of the X-ray experiments and crystal data are summarized in tables in chapter 3 section 3. Selected bond lengths and bond angles are given in these tables.

8: Bibliography

[1] Morgan, G. T.; Burstall, F. H.; *J. Chem. Soc*., **1934**, 1498.

[2] Lippard, S. J.; *Acc. Chem. Res.*, **1978**, 11, 211.

[3] Williams, J.A.G.; *Top. Curr. Chem.*, **2007**, 281, 205.

[4] McMillin D. R.; Moore, J.J.; *Coord. Chem. Rev.*, **2002**, 229, 113

[5] Breit, B.; *Chem. Eur. J.*, **2000**, 6, 1519.

[6] Chul-Ho Jun, Choong Woon Moon, and Dae-Yon Lee; *Chem. Eur. J*., **2002**, 8, 11

[7] Chassot, L.; Muller, E.; von Zelewsky, A.; *Inorg. Chem.*, **1984**, 23, 4249-4253.

[8] Maestri, M.; Sandrini, D.; Balzani, V.; Chassot, L.; Jolliet, P.; von Zelewsky, A.; *Chem. Phys. Lett.*, **1985**, 122, 375-379.

[9] Thompson, M. E.; Djurovich, P.; Lamansky, S.; Forrest, S. R.; Baldo, M. A.; Burrows, P. E.; *U.S. Patent 6,830,828*, December 14, **2004**, 74pp.

[10] Brooks, J.; Babayan, Y.; Lamansky, S.; Djurovich, P.I.; Tsyba, I.; Bau, R.; Thompson, M.E.; *Inorg. Chem.*, **2002**, 41, 3055-3066.

[11] Kvam, P. I.; Puzyk, M. V.; Balashev, K.P.; Songstad, J.; *Acta. Chem.*, **1995,** *49*, 335.

[12] Kovelenov, Y. A.; Blake, A. J.; Geroge, M. W.; Matousek, P.; Ya, M.; Mel'nikov, Parker, A. W.; Sun, Z. X.; Towrie, M.; Weinstein, J. A.; *Dalton. Trans*, **2005**, 2092.

[13] Constable, E. C.; Henney, R. P. G.; Leese, T. A.; Tocher, D. A.; *J. Chem. Soc., Chem., Commun.*, **1990**, 513-515.

[14] Cave, G. W. V.; Alcock, N. W.; Rourke, J. P.; *Organometallics*, **1999**, 18,1801-1803.

[15] Cardenas, D. J.; Echavarren, A. M.; Ramirez de Arellano, M.C.; *Organometallics*, **1999**, 18, 3337-3341.

[16] Lai, S.-W.; Che, C.-M.; *Top. Curr. Chem.*; **2004,** *241*, 27.

[17] Lu, W.; Chan, M. C. W.; Cheung, K. K.; Che, C. M.; *Organometallics*, **2001**, 20, 2477-2486.

[18] Huo, S.; Deaton, J. C.; Sowinski, A. F.; *U.S. Patent 7,029,766*, April 18, **2006,** 24pp.

[19] Ravindranathan, D.; Vezzu, D. A. K.; Bartolotti, L.; Boyle, P. D.; Huo, S.; *Inorg. Chem.*, **2010**, 49, 8922-8928.

[20] Glenna So-Ming Tong and Chi-Ming Che; *Chem. Eur. J.*, **2009**, 15, 7225 – 7237

[21] Huo, S.; Deaton, J. C.; Kondakova, M.; Rajeswaran, M.; Giesen, D.; Lenhart, W. C.; *Abstract of Papers, 234th ACS National Meeting*, Boston, MA, August 19-23, **2007,** IONR-911.

[22] Kar-Ho Wong, Michael Chi-Wang Chan, Chi-Ming Che; *Chem. Eur. J.*, 1999, 5, 10

[23] Tang, W. S.; Lu, X.-X.; Wong, K. M.-C.; Yam, V. W.-W.; *J. Mater. Chem.*, **2005**, *15*, 2714–2720.

[24] Belmore, K. A.; Vanderpool, R. A.; Tsai, J. C.; Khan, M. A.; Nicholas, K. M.; *J. Am. Chem. Soc.*, **1988**, *110*, 2004–2005.

[25] Tse, C. W.; Man, K. Y. K.; Cheng, K. W.; Mak, C. S. K.; Chan, W. K.; Liu, Z. T.; Yip, C. T.; Djuris˘ic, A. B.; *Chem. Eur. J.*, **2007**, *13*, 328–335.

[26] Peyratout, C. S.; Aldridge, T. K.; Crites, D. K.; McMillin, D. R.; *Inorg. Chem.*, **1995**, *34*, 4484–4489.

[27]Yersin, H., Ed; Wiley-VCH: Weinheim; *Highly Efficient OLEDs with Phosphorescent Materials*, **2008**.

[28] Cocchi, M.; Kalinowski, J.; Virgili, D.; Williams, J. A. G.; *Appl. Phys. Lett.*, **2008**, *92*, 113302–113304.

[29] Baldo, M. A.; Thompson, M. E.; Forrest, S. R.; *Nature*, **2000**, *403*, 750–752.

[30] Tamayo, A. B.; Garon, S.; Sajoto, T.; Djurovich, P. I.; Tsyba, I.; Bau, R.; Thompson, M. E.; *Inorg. Chem.*, **2005**, *44*, 8723–8732.

[31] Brooks, J.; Babayan, Y.; Lamansky, S.; Djurovich, P. I.; Tsyba, I.; Bau, R.; Thompson, M. E.; *Inorg. Chem.*, **2002**, *41*, 3055–3066.

[32] Quanqing Xu, Wen-fu Fu, Guiju Zhang, Zhaoyong Bian, Junfeng Zhang, Xu Han, Wenzhan Xu; *Catal. Commun.*, **2008** 10, 49–52.

[33] Vezzu, D.; Deaton, J. C.; Jones, J. S.; Bartolotti, L.; Harris, C. F.; Marchetti, A. P.; Kondakova, M.; Pike, R. D.; Huo, S.; *Inorg. Chem.*, **2010**, 49, 5107–5119.

[34] Harris, C.; Huo, S.; unpublished results **2010**.

[35] S. H. Crosby, G. J. Clarkson, J. P. Rourke,; *J. Am. Chem. Soc.*, **2009**, 131, 14142-14143.

[36] Zucca, A.; Stoccoro, S.; Cinellu, M. A.; Minghetti, G.; Manassero, M.: *Journal of the Chemical Society, Dalton Transactions: Inorganic Chemistry* **1999**, 19, 3431-3437.

[37] Bergman, R. G.; *Nature*, **2007**, *446*, 391–393.

[38] Gol'dshleger, N. F**;** Tyabin, M. B.; Shilov, A. E.; Shteinman, A. A.; *Zh. Fiz. Khim.*, **1969**, 43, 2174.

[39] Cope, A. C.; Siekman, R. W.; *J. Am. Chem. Soc.*, **1965**, 87, 3272.

[40] Cope, A. C.; Friedrich, E. C.; *J. Am. Chem. Soc.*, **1968**, 90, 909.

[41] A. D. Ryabov; *Chem. Rev.*, **1990**, *90*, 403-424.

[42] Zucca, A.; Stoccoro, S.; Cinellu, M.A.; Minghetti, G.; Manassero, M.; Sansoni, M.; *Eur. J. Inorg. Chem.*, **2002**, 3336-3346.

[43] L. Calligaro, R. A. Michelin, P. Uguagliati; *Inorg. Chim. Acta.*, **1983**, 76, 83.

[44] Marrone, A.; Re, N.; Romeo, R.; *Organometallic*, **2008**, 27, 2215-2222.

[45] Y. Tamaru, M. Kagotani, Z.-i. Yoshida; *Angew. Chem.*, **1981**, 93, 1031-1032; *Angew. Chem. Int. Ed.*, **1981**, 20, 980-981.

[46] R. P. Houghton; *Metal Complexes in Organic Chemistry*, Cambridge University Press, London, UK, 1979, 61-62.

[47] G. Minghetti, S. Stoccoro, M. A. Cinellu, B. Soro and A. Zucca; *Organometallics*, **2003**, 22, 4770-4777.

[48] A. G. Wong-Foy, L. M. Henling, M. Day, J. A. Labinger and J. E. Bercaw; *J. Mol. Catal. A: Chem.*, **2002**, 189, 3-16.

[49] Yuan-Qing Fang, Garry S. Hanan; *Synlett*, **2003**, 6, 852–854

[50] *SAINT PLUS*; Bruker Analytical X-ray Systems: Madison, WI, **2001**.

[51] *SADABS*; Bruker Analytical X-ray Systems: Madison, WI, **2001**.

[52] Sheldrick, G. M.; *Acta Crystallogr., Sect. A* **2008**, *64*, 112.